nature portfolio

Peer Review File

Neoadjuvant chemotherapy interferes with tertiary lymphoid structure formation in Epstein-Barr Virus-Associated Gastric Cancer

Corresponding Author: Professor Jiafu Ji

This file contains all reviewer reports in order by version, followed by all author rebuttals in order by version.

Version 0:

Reviewer comments:

Reviewer #1

(Remarks to the Author)
In this study, Bi et al. analyzed the largest cohort to date of locally advanced EBV-associated gastric cancer (EBVaGC) and showed, using spatial transcriptomics and single-cell analyses, that EBVaGC is characterized by enhanced tertiary lymphoid structure (TLS) formation compared with EBV-negative gastric cancer (EBVnGC), particularly at the invasive margin (IM-TLS), which was identified as a key prognostic factor. They further demonstrate that neoadjuvant 5-FU–based chemotherapy disrupts TLS formation, and that disease recurrence is associated with recruitment of aging neutrophils via the CXCR4–CXCL12 axis and chemotherapy-induced EBV reactivation, which promotes neutrophil extracellular trap formation and consequently impairs lymphocyte trafficking and TLS maturation. Overall, the authors propose IM-TLS preservation as a potential prognostic biomarker and suggest that targeting neutrophil dysfunction may represent a promising strategy to improve outcomes of neoadjuvant chemotherapy in EBVaGC.

While the suggestion that neoadjuvant chemotherapy may adversely affect outcomes in EBVaGC by modulating TLS formation through EBV reactivation is intriguing, the current dataset is largely descriptive and several major issues remain in terms of data interpretation. In particular, the manuscript lacks sufficient functional and mechanistic experiments to explain the proposed phenotypes, which substantially weakens the strength of the conclusions.

1. Although evaluating TLS in mouse cancer models is technically challenging, key findings should still be validated in at least one additional EBV-positive cancer cell line. Moreover, while the data suggesting that neutrophil NETs impair lymphocyte migration may account for the reduction in tumor-infiltrating lymphocytes, the claim that NETs suppress TLS formation and maturation appears overstated. To support this, spatial evidence in post-neoadjuvant specimens of EBVaGC demonstrating co-localization of NET-positive neutrophils around EBV-reactivated tumour cells together with a corresponding regional reduction in IM-TLS would be required. Figure 5D is important for this evidence. However, it currently lacks an integrated quantitative analysis incorporating both NET-positive neutrophils and TLS formation.

2. Regarding Figure 1, in panels 1D, 1E, 1L, 1M, 1N and 1O, the authors evaluate not only TLS density but also the abundance of mature TLSs, including primary follicle-like TLSs (PFL-TLSs) and secondary follicle-like TLSs (SFL-TLSs). However, representative histopathological images illustrating the morphological features of immature TLSs, PFL-TLSs and SFL-TLSs are not provided and should be included for clarity. Furthermore, while Figures 1R and 1S suggest that decreased IM-TLS is associated with recurrence, it remains unclear whether, in the post-neoadjuvant setting, patients with preserved IM-TLS versus those with IM-TLS loss can be distinguished by differences in EBV burden and/or the extent of NET-positive neutrophil infiltration. A more detailed analysis in this regard would be important to support the proposed mechanism.

3. Regarding Figure 2J–2M (and Figure 3D), the data indicate that, after neoadjuvant chemotherapy, GC B cells and activated DCs are decreased, whereas Treg cells and Tfh cells—both key components of TLSs—are significantly increased in terms of component abundance. The authors should clarify how the increase in Tfh cells is interpreted in the context of TLS reduction, and it would also be important to assess the proportion of $CXCL13^{+}CD8^{+}$T cells. These points highlight the need for a more quantitative and spatial evaluation of IM-TLS reduction. Moreover, given that a conclusion is that NET-forming neutrophils selectively impair TLS integrity, the authors should provide data showing whether NET-positive

neutrophils preferentially deplete B cells and/or DCs, but not Treg or Tfh cells, within IM-TLS regions.

4. Regarding Figure 3B, the data show an increase in neutrophils after neoadjuvant chemotherapy; however, the relative abundance of cDC1, CD8 Trm, and NK cells also appears to increase. The authors should clarify how these changes are interpreted in the context of disease recurrence. A more quantitative analysis of these shifts (e.g., absolute cell densities or proportions within defined regions) would be necessary to support the conclusions.

5. Regarding Figure 4 and Figure S7, Figure S7E shows that, in EBVaGC, neutrophil subsets defined by CXCR2, CXCR4 or VEGFA expression increase after neoadjuvant chemotherapy (vs treatment-naïve), whereas the ISG15$^+$ subset is not increased to the same extent as in the EBVaGC versus EBVnGC comparison. Despite this, the authors largely explain neutrophil infiltration on the basis of the CXCR4–CXCL12 axis, even though Figure 4G indicates that CXCR2-mediated interactions involve a greater number of candidate ligand–receptor pairs, which warrants more careful evaluation. In addition, the cellular sources of CXCL12 and other relevant chemokines should be identified, ideally by mIHC.
In Figure 4E, CXCR4 expression is used to define aging neutrophils; it should also be clarified whether CXCR2 is highly expressed in this subset.
Finally, in Figure S7I, aging neutrophils are defined by IRF7, MAFF, HMGA1 and BPTF, whereas Figure S7E shows that ISG15$^+$ subset is decreased in neoadjuvant-treated EBVaGC compared with neo-naïve cases. Because ISG15 is later implicated in NET formation, this apparent inconsistency should be addressed.

6. Regarding Figure 5, the authors propose that chemotherapy-induced EBV reactivation is recognized by neutrophils and triggers NET formation. However, it is unclear whether this reactivation is sensed exclusively by neutrophils or also by other immune cell populations, and this should be clarified. In Figure 5A, it should also be specified whether all genes used to define the aging neutrophil signature in Figure S7I (IRF7, MAFF, HMGA1 and BPTF) are significantly upregulated.
Finally, as noted above, validation in a single EBV-positive cancer cell line is insufficient; key findings should be confirmed in at least one additional EBV-positive cell line to strengthen the conclusions.

Minor
The description of the data presented in Figure 1P is insufficient and should be explained more clearly.

In Figure S6F, the analysis includes gastric cancers that are not EBV-positive. Therefore, the interpretation of these data in the specific context of EBVaGC should be made with caution.

In Figure S6J (neoadjuvant cohort), there appears to be no statistically significant difference. Thus, the statement that CD66b and CD20 expression are inversely correlated is not supported by the presented data and should be revised or removed.

In Figure 4A, the authors should include the list of genes used to define each of the six subpopulations.

For Figures 4K and 4M, appropriate isotype controls should be included.

Reviewer #2

(Remarks to the Author)
This manuscript compellingly investigates a novel mechanism of chemotherapy resistance by focusing on the remodeling of the immune microenvironment. It establishes a critical link between the formation of tertiary lymphoid structures (TLS) and the reactivation of the Epstein-Barr virus (EBV). Leveraging a large clinical cohort of EBVaGC to date and integrating multi-omics data, the authors demonstrate that 5-FU-based chemotherapy drives EBV lytic reactivation, which in turn triggers TLR7 signaling in neutrophils, leading to the formation of neutrophil extracellular traps (NETs) that create a physical barrier, hindering lymphocyte infiltration and compromising the anti-tumor immune response. However, several important considerations need to be addressed to strengthen the conclusions and enhance the overall robustness of the study.
1. The mechanistic data relies primarily on 5-FU (Figures 4 & 5), yet the clinical cohort received combination therapies involving platinum drugs (e.g., oxaliplatin, cisplatin). To enhance clinical relevance, the authors should determine whether platinum-based agents also induce EBV lytic reactivation (e.g., BZLF1 expression) and the subsequent neutrophil aging phenotype. It is important to clarify if this mechanism is specific to 5-FU or a general response to DNA-damaging chemotherapy.
2. The defined "aging" phenotype shares significant overlap with polymorphonuclear myeloid-derived suppressor cells (PMN-MDSCs). The authors should explicitly compare the "aging" signature with established PMN-MDSC signatures (e.g., LOX-1 expression) and senescence markers (e.g., p16, p21, β-galactosidase activity). Besides, the current data does not sufficiently distinguish whether these cells exclusively exert immune suppression via the proposed "physical barrier" (NETs) or simultaneously through other "chemical/metabolic" mechanisms (e.g., PD-L1, Arginase-1, ROS) typical of PMN-MDSCs. Perform functional assays to decouple physical exclusion from chemical suppression or exhaustion. For instance, does the inhibition of PD-1/PD-L1 or Arginase-1 or ROS restore T-cell migration in the presence of NETs?
3. The link between 5-FU, EBV, and TLR7 requires more rigorous validation. Chemotherapy can induce the release of general danger-associated molecular patterns (DAMPs), such as mtDNA, from EBV-negative cells. To control for the effects of general cell death, the authors should consider constructing stable viral knockout or cleared cell lines. In addition, hydroxychloroquine (HCQ) is a non-specific TLR7 inhibitor that also affects autophagy. Validate the mechanism using a specific TLR7 antagonist to rule out off-target effects of HCQ.
4. The evidence primarily relies on in vitro data. Although the authors acknowledge the challenges posed by the lack of immunocompetent animal models that can effectively study EBV infection, the link between viral reactivation and NETs

remains somewhat weak. To enhance the evidence, it is recommended that they conduct multiple immunohistochemistry (mIHC) analyses on NAC-treated tumor sections to co-localize EBV lytic antigens (e.g., BZLF1) with neutrophil/NET markers (CitH3, MPO) within the same microanatomical regions.
5. The retrospective comparison between NAC and surgery-upfront groups is prone to selection bias, as NAC patients often present with higher baseline tumor burden. The author should perform Propensity Score Matching (PSM) to balance baseline characteristics between the two groups. This is essential to substantiate the conclusion that NAC provides no survival benefit.
6. The effectiveness of immune checkpoint blockade (ICB) in EBVaGC represents a promising avenue for future treatment strategies. Given the viral nature of EBVaGC and the immune landscape altered by chemotherapy, the authors should discuss the implications of their findings for the enhancement of responses to existing ICBs.

Reviewer #3

(Remarks to the Author)
This manuscript investigates the impact of neoadjuvant chemotherapy on tertiary lymphoid structures (TLSs) in Epstein–Barr virus–associated gastric cancer (EBVaGC). Using a large single-center cohort combined with spatial transcriptomics, single-cell RNA sequencing, multiplex immunohistochemistry, and functional in vitro assays, the authors demonstrate that neoadjuvant chemotherapy fails to improve clinical outcomes in EBVaGC and instead disrupts invasive-margin TLSs (IM-TLSs). Mechanistically, chemotherapy induces EBV reactivation, which promotes neutrophil aging via PRR activation and CXCR4–CXCL12–mediated recruitment. These aging neutrophils form NETs around TLSs, impairing lymphocyte trafficking and TLS maturation, ultimately compromising anti-tumor immunity.
The study addresses an important and timely question at the intersection of tumor immunology, viral oncology, and treatment resistance. The presented data are interesting, and the proposed link between EBV reactivation, neutrophil aging, and TLS impairment is novel and potentially impactful. However, the manuscript is very dense, and several conceptual, methodological, and presentation-related issues should be addressed to strengthen clarity, rigor, and interpretability, particularly given that the conclusions are predominantly supported by large-scale correlative omics analyses rather than direct mechanistic evidence.
Major Comments
1. Causality between EBV reactivation and TLS disruption remains poorly mechanistically supported. While the data strongly correlate chemotherapy, EBV reactivation, neutrophil aging, NET formation, and TLS impairment, direct causal evidence in vivo is lacking. All mechanistic validation is performed in vitro. There is no animal or ex vivo tissue model demonstrating that blocking EBV reactivation, CXCR4 signaling, or NET formation restores TLS maturation. My suggestions are:
• Consider adding correlative analyses in patient tissues linking EBV lytic gene expression levels with NET density and TLS maturity.
• If feasible, include pharmacologic inhibition data (e.g., DNase I, CXCR4 blockade, or PRR inhibition) in organoid- or slice-based models.
• Quantitative multiplex immunofluorescence in patient samples—incorporating established markers of TLS maturation and functon(e.g., CD4, CD8, CD21, CD23, HEVs) with NET quantification, in larger number of patients samples rather than representative images—could strengthen this aspect. In addition, these images might support the impact on TLS development in various parts of the TME. In addition, it remains unclear whether TLS disruption is a primary driver or a secondary amplifier of immune failure. Finally, TLSs are largely treated as a binary entity despite increasing evidence of functional heterogeneity, and it is unknown whether all TLS phenotypes are equally susceptible to NET-mediated disruption.
• Explicitly acknowledge this limitation earlier in results and discussion part. Other NET-mediated immunosuppressive mechanisms (e.g., protease activity, checkpoint ligand induction) should be investigated or at least discussed.
2. The conclusion that neoadjuvant chemotherapy is ineffective in EBVaGC may be overstated, as sample size for neoadjuvant EBVaGC (n=45) is modest, regimens are heterogeneous (SOX, XELOX, DOS/POS, FLOT, FOLFOX) and pathologic complete response (pCR) rate is low but confidence intervals are not provided. My suggestions are: discuss properly your findings avoiding overstatments, provide confidence intervals for pCR and survival outcomes and discuss whether specific regimens or treatment durations showed differential effects.
3. Classification of aging neutrophils. The classification of “aging neutrophils” relies primarily on CXCR4 upregulation and transcriptomic features, raising concerns regarding definitional clarity and generalizability. Direct comparison of the proposed signature with published PMN-MDSC or senescent neutrophil gene signatures would strengthen this point. Moreover, the manuscript alternates between “aging neutrophils” and PMN-MDSC–like features without clearly defining their relationship, making it unclear whether these cells are functionally equivalent to PMN-MDSCs or represent a distinct subset. The current framing risks over-interpreting a transcriptional state as a functional lineage, which has important therapeutic implications.
Finally, given that macrophages, dendritic cells, and broader antigen-presenting cell dysfunction can independently affect TLS integrity and T cell priming, it would be important to discuss or analyze the contribution of other myeloid populations within the available transcriptomic datasets.
4. Confounding effect of tumor stage and baseline immune contexture. Although the authors state that IM-TLS is an independent prognostic factor, it remains unclear whether, patients receiving neoadjuvant chemotherapy had systematically different baseline immune architectures (e.g. lower pre-existing TLS density or maturity) and/or EBVaGC tumors selected for neoadjuvant therapy were more advanced, biologically aggressive, or anatomically unfavorable.
5. Spatial architecture. The redefinition of the invasive margin as a ±300 μm “functional invasive margin” based on spatial transcriptomics is an interesting and potentially important conceptual advance. However, its robustness and generalizability across samples remain unclear. The authors should clarify how sensitive their findings are to this spatial cutoff and whether alternative margin definitions or thresholds were tested. In addition, further explanation would help readers understand how

this functional definition could be reproduced or approximated in routine pathological or translational settings, where spatial transcriptomic data are not readily available.

Minor Comments
Clarity, structure and reporting
1) The manuscript is extremely information-dense, particularly in the Results section. Consider reducing redundancy and improving signposting to help readers follow the narrative.
2) Some Results subsections are very long and could benefit from clearer separation of descriptive vs. mechanistic findings.
3) Several figures contain a large number of panels; clearer labeling and more explicit figure legends would improve accessibility.
4) Please ensure consistent reporting of statistical tests, sample sizes, and correction methods across figures and supplementary materials. In some places, p-values are reported without clear indication of the test used.

Reviewer #4

(Remarks to the Author)
In their manuscript the authors present an in-depth analysis of Epstein-Barr virus-associated gastric carcinoma (EBVaGC). Through the use of IHC, bulk RNAseq, single-cell RNAseq and spatial transcriptomics they studied tertiary lymphoid structures (TLS) in that tumor context. The authors describe TLS enrichment in EBVaGC versus EBV negative gastric carcinoma (EBVnGC), density of TLS in the invasive margin (IM) association with better prognosis and neutrophils impairing TLS maturation via NETS and the CXCR4-CXLC12 axis.

Overall, the manuscript is extremely dense with some figures even reaching panel R or S, making hard to read the labels and to properly follow the story. The authors should try to reduce the number of panels / analyses to focus their effort on analyses that directly support their claims.

Please find major comments below:
1) While it is nicely demonstrated that neo-adjuvant chemo impairs TLS maturation in EBVaGC in both IM and TC, the link with neutrophils and relapse is less convincing. The authors base this critical part of the paper on only two patients (ST data for relapsed neoadj chemo n=2). The authors should leverage the “largest cohort of patients with locally advanced EBVaGC to date” to robustly quantify neutrophils and evaluate their impact on TLS maturation and relapsed status with an appropriate number of patients.

2) Similarly, the claim that Nets producing neutrophils impairing TLS maturation in the IM, should be investigated with enough power as well. What proportion of immature TLS have Nets? Are there mature TLS with NETs? Do patients with TLS and NETs have worse outcome? The authors should try to disentangle they well known immunosuppressor effect of neutrophils (are usually anti-correlated with B cells, T cells etc…) from there impact on TLS maturation.

Version 1:

Reviewer comments:

Reviewer #1

(Remarks to the Author)
I thank the authors for their careful and comprehensive responses to my comments. The revised manuscript has been substantially improved by the addition of functional validation experiments, an independent EBV-positive cell line, expanded spatial quantitative analyses, representative primary data, and clearer mechanistic interpretation. The authors have also appropriately revised or removed unsupported analyses and have addressed the major concerns raised during review.

Overall, I consider that the revised manuscript adequately addresses my previous concerns. I have no further major comments and support publication.

Reviewer #2

(Remarks to the Author)
The authors have fully addressed my previous comments. The manuscript is significantly improved and ready for publication. I recommend acceptance.

Reviewer #3

(Remarks to the Author)
The revised manuscript has been substantially improved and many of the concerns raised in the previous round have been addressed. In particular, the addition of spatial mIHC analyses, validation in an independent EBV-positive cell line, clarification of the aging neutrophil phenotype, and implementation of propensity score matching have strengthened both the mechanistic and clinical aspects of the study.

However, several points should still be considered to further strengthen the central conclusions and improve the interpretation of the data.
1. The revised analyses provide stronger spatial evidence linking EBV reactivation, NET accumulation, and impaired TLS maturation. Nevertheless, direct evidence demonstrating that inhibition of NET formation, CXCR4 signaling, or EBV reactivation restores TLS maturation in an intact tissue context is still lacking. For this reason, some of the causal statements throughout the manuscript should be moderated.
In addition, the proposed model would benefit from a more quantitative assessment of NET distribution across different TLS maturation stages. Specifically, it would be informative to report the prevalence or density of NET-positive neutrophils in early TLSs, primary follicle-like TLSs, and secondary follicle-like TLSs. Such an analysis would provide a more direct assessment of the relationship between NET accumulation and TLS maturation. Additionally, if data are available, spatial analyses examining the relationship between NET-rich regions and the local abundance of key TLS-associated populations, particularly B cells and dendritic cells, would further strengthen the proposed mechanism.
2. The manuscript demonstrates associations between NET accumulation, TLS disruption, and recurrence. It would be valuable to determine whether NET burden retains prognostic significance after adjustment for TLS-related variables. If feasible, a multivariable analysis incorporating NET density together with IM-TLS status/maturity and relevant clinicopathological variables would help clarify whether NET accumulation contributes prognostic information beyond TLS measurements alone.
3. While the revised manuscript provides substantially improved spatial and mechanistic evidence, the causal relationship between NET accumulation and TLS maturation remains largely inferred from spatial associations and in vitro experiments. I encourage the authors to acknowledge this limitation more explicitly and to clearly distinguish between observations directly supported by the data and mechanistic interpretations that remain speculative.

Reviewer #4

(Remarks to the Author)
The authors have significantly improved their manuscript and appropriately addressed my comments.

Version 2:

Reviewer comments:

Reviewer #3

(Remarks to the Author)
The authors have substantially improved the manuscript and have satisfactorily addressed all of my comments.

Reviewer #1 (Remarks to the Author):

In this study, Bi et al. analyzed the largest cohort to date of locally advanced EBV-associated gastric cancer (EBVaGC) and showed, using spatial transcriptomics and single-cell analyses, that EBVaGC is characterized by enhanced tertiary lymphoid structure (TLS) formation compared with EBV-negative gastric cancer (EBVnGC), particularly at the invasive margin (IM-TLS), which was identified as a key prognostic factor. They further demonstrate that neoadjuvant 5-FU–based chemotherapy disrupts TLS formation, and that disease recurrence is associated with recruitment of aging neutrophils via the CXCR4–CXCL12 axis and chemotherapy-induced EBV reactivation, which promotes neutrophil extracellular trap formation and consequently impairs lymphocyte trafficking and TLS maturation. Overall, the authors propose IM-TLS preservation as a potential prognostic biomarker and suggest that targeting neutrophil dysfunction may represent a promising strategy to improve outcomes of neoadjuvant chemotherapy in EBVaGC.

While the suggestion that neoadjuvant chemotherapy may adversely affect outcomes in EBVaGC by modulating TLS formation through EBV reactivation is intriguing, the current dataset is largely descriptive and several major issues remain in terms of data interpretation. In particular, the manuscript lacks sufficient functional and mechanistic experiments to explain the proposed phenotypes, which substantially weakens the strength of the conclusions.

Response:

We sincerely thank Reviewer #1 for the highly constructive, rigorous, and insightful evaluation of our manuscript. We fully agree with your overarching assessment that the previous version of the manuscript required stronger functional and mechanistic support to substantiate our descriptive findings. Guided by your valuable suggestions, we have conducted extensive additional experiments, integrated new multi-omic spatial analyses, and comprehensively revised our manuscript to ensure robust data interpretation. The major improvements in this revision include:

We have replicated key *in vitro* functional assays using an additional EBV-positive cell line (C666-1) and performed chemotaxis assays using flow-sorted/magnetically isolated immune cells. These new data definitively demonstrate that NETs act as a non-selective physical barricade impeding lymphocyte trafficking.

To provide direct *in situ* quantitative evidence, we perform a custom 10-plex mIHC panel (panel 3: PanCK/BZLF1/CD66b/MPO/CitH3/CD20/CD23/α-SMA/CXCL12/CXCR4) in a large cohort comprising 216 strictly annotated FFPE specimens (including 38 EBVaGC and 178 EBVnGC cases). We mapped the spatial co-localization of EBV reactivation, NET accumulation, TLS maturation impedance, and CXCL12-producing cellular sources at the invasive margin.

We have re-evaluated our spatial transcriptomic data to clarify the paradoxical compositional shifts within the TLS (e.g., Tfh/Treg enrichment). We demonstrate that these shifts reflect a "frustrated" immune state, combined with differential chemotherapeutic cytotoxicity, rather than selective NET gating.

To improved data rigor, we have incorporated representative histological images, flow cytometry isotype controls, and high-resolution sub-cluster gene lists. Additionally, we removed previously unsupported supplementary data to keep our narrative scientifically tight and rigorous.

Furthermore, we have systematically addressed the critical issues you raised by incorporating them into the Discussion section of the revised manuscript. By explicitly confronting these theoretical and mechanistic queries, we have substantially expanded the depth and scope of our discussion,

providing a much more comprehensive and nuanced interpretation of our findings.

We firmly believe that your critiques have fundamentally elevated the mechanistic depth and overall quality of this manuscript. Please find our detailed point-by-point responses to your comments below.

1. Although evaluating TLS in mouse cancer models is technically challenging, key findings should still be validated in at least one additional EBV-positive cancer cell line.

Response:

We have replicated the key *in vitro* experiments originally performed in the SNU719 gastric cancer cell line using the EBV-positive nasopharyngeal carcinoma cell line, C666-1. The validation results consistently support our primary findings:

① Induction of EBV reactivation: Both Western blotting and immunocytochemistry assays confirmed that treatment with various chemotherapeutic agents (5-FU, L-OHP, and PTX) successfully induced the expression of the EBV reactivation-associated transcription factor, BZLF1, in C666-1 tumor cells, with 5-FU demonstrating the most prominent induction effect (Fig. S9E, F).

② Neutrophil recruitment and activation: We subsequently performed indirect co-culture assays using neutrophils and the chemo-treated C666-1 cells. Compared to the controls, neutrophils co-cultured with the chemo-treated C666-1 cells exhibited: upregulated surface expression of CXCR4, as determined by flow cytometry (Fig. S8D), enhanced chemotactic migration towards a CXCL12 gradient, as demonstrated in Transwell migration assays (Fig. S8F), an augmented capacity for NET release, as evidenced by *in vitro* NET formation assays (Fig. S9C).

③ Impairment of lymphocyte migration: Importantly, Transwell assays further confirmed that these activated neutrophils (co-cultured with 5-FU-treated C666-1 cells) effectively hindered the chemotactic migration of lymphocytes towards a CXCL13 gradient (Fig. S10H).

In summary, these data from the C666-1 cell line are highly consistent with those from the SNU719 cell line, further validating our core mechanistic axis.

Moreover, while the data suggesting that neutrophil NETs impair lymphocyte migration may account for the reduction in tumor-infiltrating lymphocytes, the claim that NETs suppress TLS formation and maturation appears overstated. To support this, spatial evidence in post-neoadjuvant specimens of EBVaGC demonstrating co-localization of NET-positive neutrophils around EBV-reactivated tumour cells together with a corresponding regional reduction in IM-TLS would be required. Figure 5D is important for this evidence. However, it currently lacks an integrated quantitative analysis incorporating both NET-positive neutrophils and TLS formation.

Response:

To address your concern and substantiate our findings, we have provided the requested spatial evidence and performed an integrated quantitative analysis. Specifically, we utilized multiplex immunohistochemistry to spatially co-localize EBV reactivation, NETs, and IM-TLSs (revised Fig. 5J). The spatial evidence visually demonstrates a distinct accumulation of NET-releasing neutrophils ($CD66b^+MPO^+CitH3^+$) at the periphery of early IM-TLSs (IM-eTLSs), accompanied by the presence of adjacent $BZLF1^+$ tumor cells (implying EBV reactivation).

Furthermore, to robustly support these observations, we conducted an integrated quantitative analysis evaluating the correlations and spatial distances among the degree of EBV reactivation, NET density, and IM-TLS maturation status at the tumor invasive margin:

① Correlation analysis: In post-neoadjuvant samples, the relapsed group exhibited a significant positive correlation between the proportion of $BZLF1^+$ tumor cells and the density of NET-releasing

neutrophils at the invasive margin. Importantly, the ratio of mTLS area to total TLS area was significantly negatively correlated with both the proportion of $BZLF1^+$ tumor cells and the density of NET-releasing neutrophils (revised Fig. 5K).

② Spatial distance analysis: The spatial distance between $BZLF1^+$ tumor cells and NET-releasing neutrophils was significantly shorter compared to that of $BZLF1^-$ tumor cells (Fig. S10D). Moreover, a spatial gradient analysis surrounding the NET-releasing neutrophils demonstrated that the proportion of $BZLF1^+$ tumor cells peaked in their immediate vicinity (0-20μm) (Fig. S10E).

③ Comparison of NET-releasing neutrophil density around TLSs of varying maturity: In the post-neoadjuvant relapsed EBVaGC group, the density of NET-releasing neutrophils at the periphery of eTLSs (within ±100μm from TLS boundaries) was significantly higher than that around mTLSs. This trend was consistently observed in both the post-neoadjuvant non-relapsed EBVaGC and treatment-naïve EBVaGC groups. However, this trend was completely absent in EBVnGC groups (Fig. S10F).

Together, these newly integrated spatial and quantitative analyses strongly support our conclusion that NETs, driven by EBV reactivation, spatially accumulate and impair TLS maturation.

2. Regarding Figure 1, in panels 1D, 1E, 1L, 1M, 1N and 1O, the authors evaluate not only TLS density but also the abundance of mature TLSs, including primary follicle-like TLSs (PFL-TLSs) and secondary follicle-like TLSs (SFL-TLSs). However, representative histopathological images illustrating the morphological features of immature TLSs, PFL-TLSs and SFL-TLSs are not provided and should be included for clarity.

Response:

To provide clear visual references for the morphological features of TLSs at different maturation stages, we have now included representative H&E images illustrating early TLSs, PFL-TLSs, and SFL-TLSs. These images have been incorporated as revised Figure 1D in the revised manuscript.

Furthermore, while Figures 1R and 1S suggest that decreased IM-TLS is associated with recurrence, it remains unclear whether, in the post-neoadjuvant setting, patients with preserved IM-TLS versus those with IM-TLS loss can be distinguished by differences in EBV burden and/or the extent of NET-positive neutrophil infiltration. A more detailed analysis in this regard would be important to support the proposed mechanism.

Response:

We further analyzed our mIHC data (panel 3) to evaluate the differences in viral reactivation burden and NET-positive neutrophil infiltration at the invasive margin. In the post-neoadjuvant setting, patients with IM-TLS loss exhibited a significantly higher density of NET-releasing neutrophils at the invasive margin compared to those with preserved IM-TLS (Fig. S10B). Additionally, the viral reactivation burden (evaluated by the proportion of $BZLF1^+$ tumor cells) showed an upward trend in patients with IM-TLS loss, although this difference did not reach statistical significance (Fig. S10C). By contrast, in the treatment-naïve cohort, there is no significance in NET-releasing neutrophil density and viral reactivation burden at the invasive margin between the two groups (Fig. S10B, C). These findings further support our proposed mechanism: the loss of IM-TLS is closely associated with an enhanced accumulation of NET-releasing neutrophils, a phenomenon that is particularly prominent following neoadjuvant chemotherapy.

3. Regarding Figure 2J–2M (and Figure 3D), the data indicate that, after neoadjuvant chemotherapy,

GC B cells and activated DCs are decreased, whereas Treg cells and Tfh cells—both key components of TLSs—are significantly increased in terms of component abundance. The authors should clarify how the increase in Tfh cells is interpreted in the context of TLS reduction, and it would also be important to assess the proportion of $CXCL13^+CD8^+$T cells. These points highlight the need for a more quantitative and spatial evaluation of IM-TLS reduction. Moreover, given that a conclusion is that NET-forming neutrophils selectively impair TLS integrity, the authors should provide data showing whether NET-positive neutrophils preferentially deplete B cells and/or DCs, but not Treg or Tfh cells, within IM-TLS regions.

Response:

Following your constructive suggestions, we have now quantified the spatial proportion of $CXCL13^+CD8^+$ T cells. Furthermore, we have provided additional spatial distribution data and performed chemotaxis assays using flow-sorted or magnetically separated immune cells to robustly demonstrate that the physical barrier effect of NETs is non-selective. We have also extensively revised our manuscript to explicitly explain the paradoxical phenomenon of Tfh/Treg cell enrichment in the context of overall TLS reduction. We address your specific points in detail below:

① Assessment of $CXCL13^+CD8^+$ T cells in spatial transcriptome data

As requested, we evaluated the relative spatial abundance of $CXCL13^+CD8^+$ T cells, which are well-known early initiators of TLS formation. In our scRNA-seq data, high CXCL13 expression was predominantly observed in the CD8T_NME2, Cycling_T, and CD8T_Tex subsets. As depicted in the bubble plot (Author Response Figure. 1A), these three clusters represent effector $CD8^+$ T cells transitioning from an early proliferative-exhausted state to terminal exhaustion.

We merged these three subsets to define the overall $CXCL13^+CD8^+$ T cell population. When comparing relative abundances between groups, we observed that following NAC, the abundance of $CXCL13^+CD8^+$ T cells showed no significant overall change in the IM spots, but decreased drastically specifically within the IM-TLS spots (revised Fig. 2J, L). This discrepancy is closely tied to the proliferative state of these cells. Inside the TLS, antigen-engaged $CD8^+$ T cells undergo robust clonal expansion to exert their functions and secrete CXCL13. Because chemotherapy preferentially targets rapidly dividing cells, these actively proliferating T cells within the TLS are directly eradicated. In contrast, the lack of significant difference in the general IM region reflects a dynamic equilibrium between ongoing cellular recruitment and chemotherapy-induced destruction.

When comparing patient outcomes within the neoadjuvant group, we observed that relapsed patients had significantly higher levels of $CXCL13^+CD8^+$ T cells in the general IM, indicating a more severely exhausted overall tumor microenvironment (revised Fig. 2K, M). Interestingly, no such difference was found inside the IM-TLS compartment. This lack of prognostic difference within the IM-TLS reflects two phenomena: First, chemotherapy indiscriminately eradicates the dividing $CD8^+$ T cells inside the TLS down to a minimal baseline in all patients, thereby erasing any potential outcome-driven differences in this specific compartment. Second, it corroborates the non-selective barrier effect of NETs—even though there is a higher abundance of these T cells in the broader IM region, they are physically hindered from infiltrating the IM-TLS.

② Explaining Tfh/Treg enrichment in the context of TLS reduction and the non-selective nature of NETs

By integrating spatial transcriptomic analyses with new *in vitro* experiments, we investigated whether NETs exert selective gating. By defining "NET spots" based on the relative abundance of neutrophils, we performed a spatial gradient analysis for various cell subtypes at the periphery of

IM-TLSs. The results revealed that all evaluated immune cell types universally accumulated directly adjacent to the NET spots, indicating a non-discriminatory physical blockade (Author Response Figure. 1B). Further, we performed Transwell migration assays using flow-sorted $CD3^{-}CD20^{+}$ B cells, $CD3^{+}CD8^{+}$ T cells, and $CD3^{+}CD4^{+}$ T cells (Author Response Figure. 1C), and magnetically separated pan-DCs (MojoSort™ Human Pan DC Isolation Kit, BioLegend, Cat#480143). Consistent with the spatial data, the migration of all tested cell types was similarly obstructed by NETs, confirming the complete absence of cell-type selectivity (Author Response Figure. 1D).

Regarding the seemingly contradictory reduction of overall TLS structures alongside an increase in Tfh and Treg cells, we attribute this phenomenon to differential chemotherapeutic cytotoxicity, biological lifespans and antigen-dependency. Chemotherapy exerts a massive killing effect on rapidly proliferating cells while largely sparing terminally differentiated, tissue-resident cells. Within the TLS, GC B cells and actively expanding pre-exhausted T cells (such as $CXCL13^{+}CD8^{+}$ T cells) possess the highest proliferation rates. Consequently, they suffer massive direct apoptosis due to chemotherapy toxicity. Conversely, mature DCs, Tfh, and Treg cells are terminally differentiated, slow-cycling tissue-resident cells that endure the chemotherapy relatively unscathed. Besides, GC B cells are among the most rapidly dividing cells in mammals and exist in a "pro-apoptotic default state"[1]. They absolutely rely on continuous antigen presentation by DCs and FDCs to survive; without it, they undergo rapid apoptosis within hours. In stark contrast, effector Tfh cells and Tregs are relatively long-lived, capable of residing in local tissues for weeks to months[2,3].

Therefore, when chemotherapy disrupts the TLS structure, the GC B cell pool rapidly collapses and undergoes massive apoptosis, whereas the relatively long-lived Tfh and Treg cells are left stranded in the tissue. Consequently, the observed "increase" in Tfh/Treg spatial abundance is not a result of selective gating by NET barriers, but rather a relative spatial enrichment (an increased proportion in the spatial deconvolution prediction scores) mathematically driven by the dramatic loss of the B cell compartment.

Collectively, these data demonstrate that chemotherapy-induced NETs function as a non-selective, viscous physical barrier. The observed shifts in cellular compartmentalization are not the result of selective gating by NETs. Instead, they represent the combined consequences of differential chemotherapeutic toxicity on cells with varying proliferative capacities, differing dependencies on continuous antigen presentation, and the universal accumulation of cells physically blocked by NETs. This dynamic is ultimately reflected as a relative shift in the spatial deconvolution proportions.

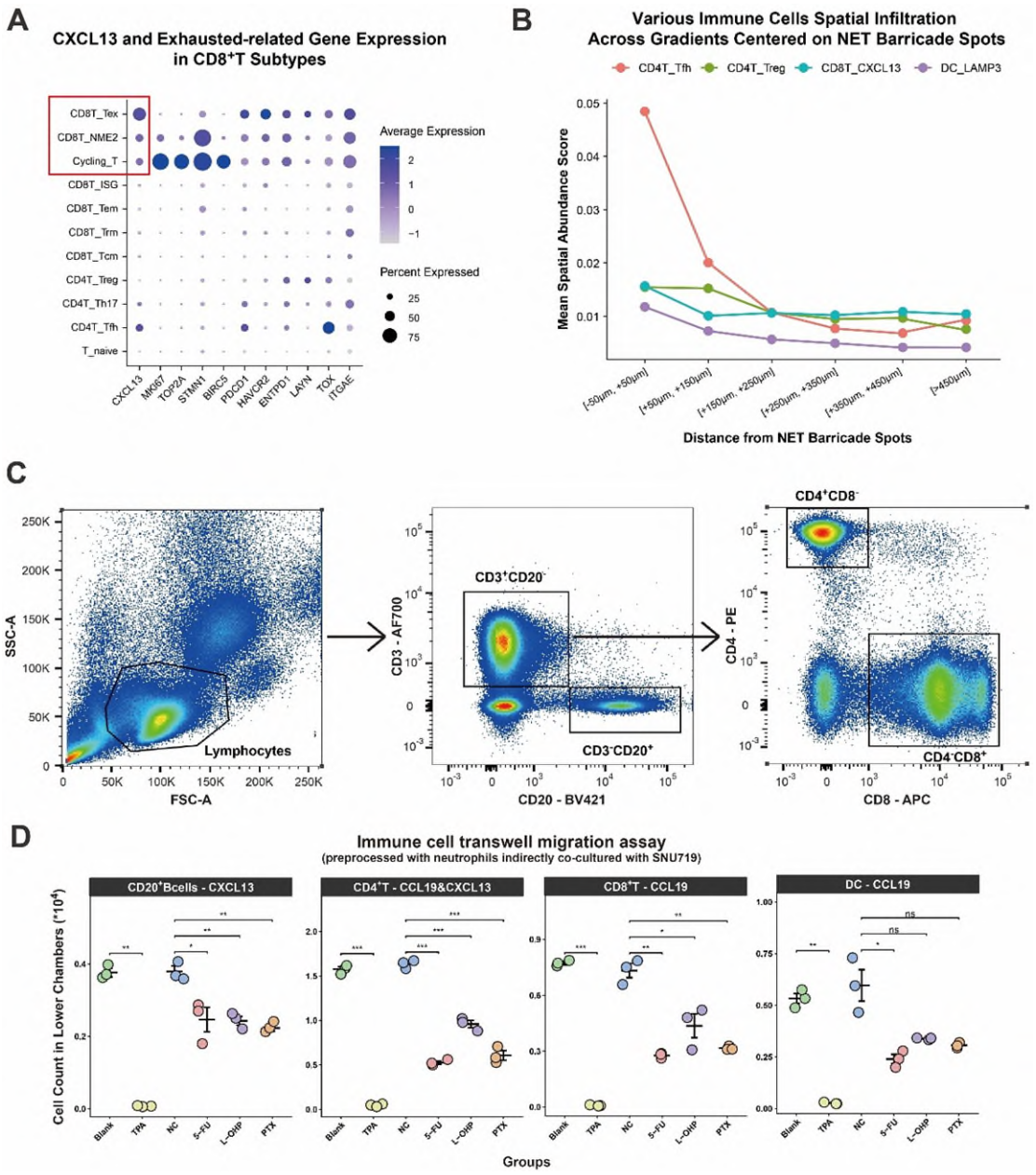

Author Response Figure 1. Evaluation of CXCL13^{+}CD8^{+} T cells and validation of the non-selective physical barrier effect of NETs.

(A) Bubble plot showing the expression levels of CXCL13 and exhaustion-related genes across various CD8^{+} T cell subclusters based on scRNA-seq data. The red box highlights the CD8T_Tex, CD8T_NME2, and Cycling_T subsets, which predominantly express CXCL13 and were merged to represent the overall CXCL13^{+}CD8^{+} T cell population.

(B) Spatial gradient analysis of various immune cell subtypes (Tfh, Treg, CXCL13^{+}CD8^{+} T cells, and mature DCs) centered on defined NET barricade spots. All evaluated immune cells universally accumulated at the immediate periphery of the NET spots (distance: [-50μm, +50μm]), indicating a non-discriminatory spatial blockade.

(C) Flow cytometry gating strategy for sorting specific immune cell populations, including CD3^{-}CD20^{+} B cells, CD3^{+}CD8^{+} T cells, and CD3^{+}CD4^{+} T cells, for downstream functional assays.

(D) *In vitro* Transwell migration assays demonstrating the absence of cell-type selectivity by NETs.

Flow-sorted lymphocytes and magnetically isolated pan-DCs were subjected to chemotaxis towards specific chemokine gradients (CXCL13 and/or CCL19). The data consistently show that pre-processing with neutrophils indirectly co-cultured with chemo-treated SNU719 cells (particularly in the 5-FU group) similarly obstructs the migration of all tested immune cell types, confirming that NETs act as a non-selective physical barricade.

Referrence

1 Victora, G. D. & Nussenzweig, M. C. Germinal Centers. *Annual Review of Immunology* **40**, 413-442, doi:10.1146/annurev-immunol-120419-022408 (2022).

2 Crotty, S. T Follicular Helper Cell Biology: A Decade of Discovery and Diseases. *Immunity* **50**, 1132-1148, doi:10.1016/j.immuni.2019.04.011 (2019).

3 Muñoz-Rojas, A. R. & Mathis, D. Tissue regulatory T cells: regulatory chameleons. *Nature Reviews Immunology* **21**, 597-611, doi:10.1038/s41577-021-00519-w (2021).

4. Regarding Figure 3B, the data show an increase in neutrophils after neoadjuvant chemotherapy; however, the relative abundance of cDC1, CD8 Trm, and NK cells also appears to increase. The authors should clarify how these changes are interpreted in the context of disease recurrence. A more quantitative analysis of these shifts (e.g., absolute cell densities or proportions within defined regions) would be necessary to support the conclusions.

Response:

Since Figure 3B is derived from spatial deconvolution scores exclusively within the structurally defined IM-TLS regions, it already intrinsically reflects the shifts in cellular proportions within this specific spatial compartment. To address the reviewer's request for a more quantitative presentation, we have now extracted the exact statistical metrics (adjusted P-values and Log2FC) for these subsets and provided a quantitative list as below (Author Response Table 1).

Author Response Table 1. Differential cellular composition analysis between prognosis groups in IM-TLS spots of neoadjuvant chemotherapy samples

Celltype	adjusted P-values	Log2FC	Enrichment
DC_cDC1	3.50E-24	1.877665479	Enriched_in_Relapsed
Fibro_mCAF_POSTN	1.14E-26	1.223223138	Enriched_in_Relapsed
CD8T_Tem	1.72E-08	1.156525659	Enriched_in_Relapsed
DC_pDC	1.03E-25	1.049877331	Enriched_in_Relapsed
NK_CD56	1.97E-20	1.048470889	Enriched_in_Relapsed
Neutrophils	8.57E-12	0.883365266	Enriched_in_Relapsed
T_naive	1.93E-11	0.643492399	Enriched_in_Relapsed
B_Memory	0.00158	-0.58617041	Enriched_in_Non-relapsed
Macro_HSPA1A	3.69E-06	-0.66570475	Enriched_in_Non-relapsed
Cycling_stromal	0.000186	-0.85826307	Enriched_in_Non-relapsed
Fibro_CXCL12	1.73E-07	-0.93861703	Enriched_in_Non-relapsed
B_Mem_Atypical	4.38E-06	-0.97865151	Enriched_in_Non-relapsed
EC_lymphatic	5.65E-06	-1.07918439	Enriched_in_Non-relapsed
PB_IgA_Igλ	5.76E-29	-1.26896537	Enriched_in_Non-relapsed
PB_IgG	1.28E-26	-1.52113196	Enriched_in_Non-relapsed
Macro_C1QA	1.05E-09	-2.11859001	Enriched_in_Non-relapsed
Fibro_mCAF_CTHRC1	0.000154	-2.27018888	Enriched_in_Non-relapsed

Biologically, we attribute the enrichment of these seemingly "beneficial" cells in patients who ultimately relapsed to a combination of mathematical compositional shifts, arrested immune maturation, and the unique microenvironmental context of the relapsed tumor.

While these subsets are spatially enriched in the relapsed IM-TLS, a closer examination of their phenotypic states reveals that they are not the fully mature, optimally activated effector cells required for robust anti-tumor immunity. Although DC_cDC1 is relatively enriched in relapsed patients, it is critical to note that the fully mature, highly costimulatory DC-LAMP3 ($LAMP3^+$ mature DCs) subset is not enriched. The accumulation of cDC1 without matching terminal activation suggests an arrested maturation process. They are recruited to the site but fail to receive the necessary licensing signals to become effective antigen-presenting nodes within a functional TLS. The enriched NK subset is NK_CD56. In the tumor microenvironment, $CD56^+$ NK cells often represent a less mature or more regulatory phenotype, whereas the terminally differentiated, highly cytotoxic NK_CD16 subset is noticeably absent from this relapsed enrichment signature. CD8T_Tem (effector memory T cells) are resting memory cells. Without a structurally sound TLS containing fully activated DCs and Tfh cells to re-activate them, their mere spatial presence in the tissue does not translate to active tumor killing.

Spatial deconvolution proportions represent compositional (zero-sum) data. As shown in the left side of the volcano plot (Fig. 3B), the non-relapsed group is strongly characterized by the enrichment of a robust humoral immune core (e.g., B_Memory, B_Mem_Atypical, PB_IgA_Igλ, PB_IgG). In relapsed patients, this critical B cell memory machinery is largely defective or collapsed. Mathematically, the profound absence of this dominant B-cell compartment in relapsed patients passively inflates the relative predicted proportions of the remaining myeloid and innate lymphoid cells (like cDC1 and NK_CD56) that are stranded in the surroundings.

Crucially, these subsets in the relapsed group are co-enriched alongside a massive infiltration of Neutrophils (the most significantly enriched subset in Fig. 3B). This indicates that the relapsed IM-TLS is trapped in a state of chronic, unresolved innate inflammation. The recruited DCs, NK cells, and resting Tem cells are sequestered in a hostile, highly viscous NET-rich barricade, rendering them structurally incapable of organizing into a functional adaptive immune hub.

In summary, the enrichment of these cells in relapsed patients does not reflect an effective anti-tumor response, but rather highlights a "frustrated" immune state: innate cells and memory T cells are recruited to the tumor margin but are functionally arrested, lacking terminal activation, and physically embedded within an immunosuppressive neutrophil-dominated barricade.

5. Regarding Figure 4 and Figure S7, Figure S7E shows that, in EBVaGC, neutrophil subsets defined by CXCR2, CXCR4 or VEGFA expression increase after neoadjuvant chemotherapy (vs treatment-naïve), whereas the $ISG15^+$ subset is not increased to the same extent as in the EBVaGC versus EBVnGC comparison. Despite this, the authors largely explain neutrophil infiltration on the basis of the CXCR4–CXCL12 axis, even though Figure 4G indicates that CXCR2-mediated interactions involve a greater number of candidate ligand–receptor pairs, which warrants more careful evaluation. In addition, the cellular sources of CXCL12 and other relevant chemokines should be identified, ideally by mIHC.

In Figure 4E, CXCR4 expression is used to define aging neutrophils; it should also be clarified whether CXCR2 is highly expressed in this subset.

Response:

We address your specific points as follows:

① Identification of the cellular sources of CXCL12

Our single-cell transcriptomic analysis initially revealed that CXCL12 is primarily expressed by stromal cells (revised Fig. S7K). To validate this at the spatial protein level, we performed mIHC staining to quantify CXCL12 expression across epithelial cells (PanCK$^+$), stromal cells (α-SMA$^+$), and immune cells (PanCK$^-$α-SMA$^-$). The quantitative results confirmed that the proportion of CXCL12$^+$ stromal cells is significantly higher than that of epithelial and immune cells (revised Fig. S7L). Furthermore, spatial gradient analysis of the mIHC data demonstrated that the density of CXCL12$^+$ stromal cells peaked in the immediate vicinity of aging neutrophils (CXCR4$^+$CD66b$^+$), with the density progressively decreasing as the distance increased (revised Fig. S7N). Importantly, mIHC staining further illustrated that these CXCL12$^+$α-SMA$^+$ stromal cells are predominantly localized around the periphery of the IM-TLS (revised Fig. 4H, revised Fig. S7M). Collectively, these multi-omics data identify α-SMA$^+$ stromal cells as the primary source of CXCL12 within the IM-TLS microenvironment.

② Clarification of CXCR2 expression in aging subsets and rationale for focusing on the CXCR4-CXCL12 axis

As illustrated in our pseudotime trajectory analysis (Fig. 4C, D), CXCR2 expression gradually decreases as neutrophils transition from the initial Neu_CXCR2 state toward the aging phenotypes. Specifically, within the aging subpopulations, those located earlier in the differentiation trajectory (i.e., closer to the inflammatory phenotype, such as the Neu_CXCR4 subset) still retain partial CXCR2 expression. However, as the cells progress toward the terminal end of the trajectory (such as the Neu_VEGFA and Neu_ISG15 subsets), CXCR2 expression is nearly entirely lost.

This dynamic expression pattern perfectly aligns with the well-documented biological process of neutrophil aging *in vivo*, which is canonically characterized by the progressive upregulation of CXCR4 and the concomitant downregulation of CXCR2. This biological progression explains our mechanistic focus: While CXCR2-mediated interactions indeed involve a broader array of ligand-receptor pairs that primarily govern the initial recruitment of inflammatory neutrophils, the CXCR4-CXCL12 axis is biologically critical for the retention, spatial positioning, and accumulation of the aging neutrophils within the specific stromal niche at the IM-TLS periphery. Thus, the CXCR4-CXCL12 axis is the key functional driver for the specific aging phenotype emphasized in our study.

Finally, in Figure S7I, aging neutrophils are defined by IRF7, MAFF, HMGA1 and BPTF, whereas Figure S7E shows that ISG15$^+$ subset is decreased in neoadjuvant-treated EBVaGC compared with neo-naïve cases. Because ISG15 is later implicated in NET formation, this apparent inconsistency should be addressed.

Response:

This insightful question provides an excellent opportunity for us to clarify the subtype dynamics and the specific functional distribution of these TFs. First, we apologize for any ambiguity in our text. Although our study discusses the virus-induced neutrophil aging phenotype—and the nomenclature of the Neu_ISG15 subtype is typically associated with the interferon pathway responding to viral infections—our functional focus was never solely on the isolated Neu_ISG15 subtype, but rather on the aging neutrophil population as a whole.

The aging neutrophil (Neu_aging) was defined by their functionally enriched pathways (Figure 4B). Three subtypes (Neu_CXCR4, Neu_ISG15, and Neu_VEGFA) are collectively categorized under this phenotype, rather than referring to any single subset. Furthermore, based on the developmental

trajectory and the continuous expression of signature genes (e.g., CXCR4, SELL) (Figure 4C-E), there is a clear evolutionary path from the transitional state (Neu_CXCR4) toward the terminal states (Neu_ISG15 and Neu_VEGFA). When comparing the neutrophil subtype proportions between treatment groups, the overall proportion of the aging state (Neu_CXCR4, Neu_ISG15, and Neu_VEGFA) is elevated in the neoadjuvant group (Figure S7E).

To further address your concern, we re-evaluated the RSS at the finer 6-subtype resolution. As demonstrated in Author Response Figure 2, these four key TFs are widely shared across the three subsets constituting the Neu_aging meta-state. HMGA1 is significantly enriched in Neu_CXCR4 and Neu_VEGFA. IRF7 is enriched in Neu_ISG15 and Neu_VEGFA. BPTF and MAFF are enriched in both Neu_ISG15 and Neu_VEGFA.

This high-resolution result explicitly refutes the notion that these TFs (and their associated NET-secreting functions) are exclusively restricted to the Neu_ISG15 subtype. Instead, they constitute a shared transcriptional program driving the overarching aging phenotype. We hope this explanation thoroughly addresses your concern regarding the consistency of our data.

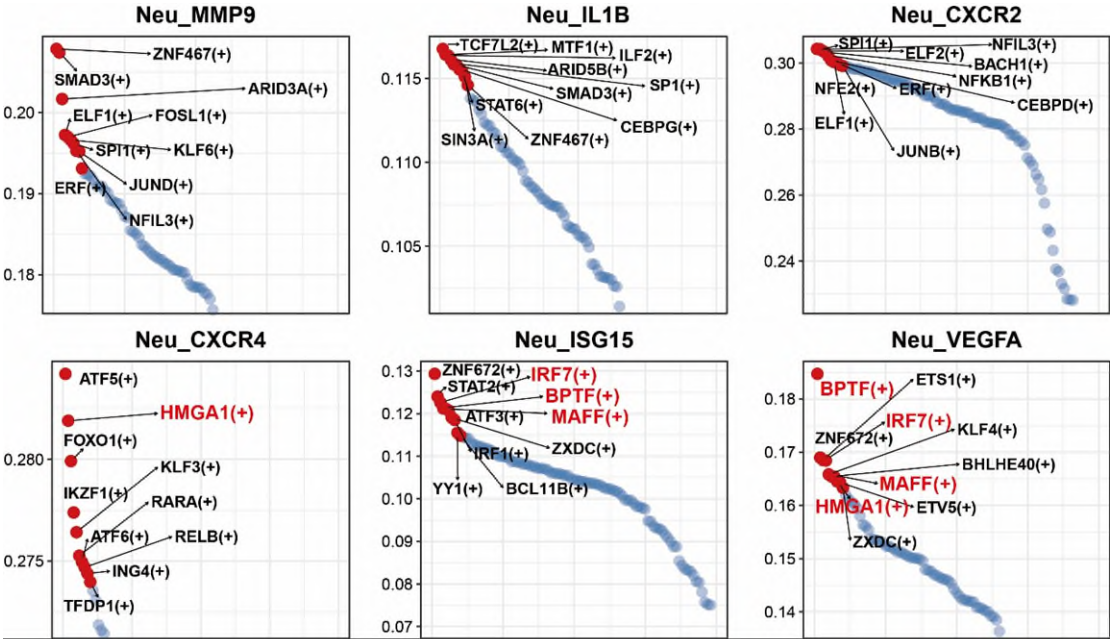

Author Response Figure 2. Transcription factor analysis showing the top RSS-ranking regulons for the six neutrophil subtypes.

6. Regarding Figure 5, the authors propose that chemotherapy-induced EBV reactivation is recognized by neutrophils and triggers NET formation. However, it is unclear whether this reactivation is sensed exclusively by neutrophils or also by other immune cell populations, and this should be clarified. In Figure 5A, it should also be specified whether all genes used to define the aging neutrophil signature in Figure S7I (IRF7, MAFF, HMGA1 and BPTF) are significantly upregulated.

Finally, as noted above, validation in a single EBV-positive cancer cell line is insufficient; key findings should be confirmed in at least one additional EBV-positive cell line to strengthen the conclusions.

Response:

We have now provided new data regarding the sensing of EBV reactivation by other immune cells

and validating the expression of the aging neutrophil-specific transcription factors. We address each point in detail below.

① Exploring other immune cell responding to EBV reactivation in mIHC data

We completely agree that the sensing of chemotherapy-induced EBV reactivation is not exclusive to neutrophils. Biologically, viral components and damage-associated molecular patterns (DAMPs) can be recognized by various pattern recognition receptors (PRRs) that are widely expressed on multiple immune cell populations.

Our mechanistic focus on neutrophils in this study was not based on an assumption of exclusivity, but rather driven by our striking spatial and clinical observations. As demonstrated in Figure 3A and 3B of the manuscript, neutrophils showed significant enrichment at the invasive margin following neoadjuvant chemotherapy, particularly in patients who experienced relapse.

To further clarify whether other key immune effector cells exhibit similar population-level responses to EBV reactivation, we utilized our mIHC cohort (panel1) to quantify the absolute spatial densities of $CD8^+$ T cells and $CD68^+$ macrophages specifically at the invasive margin. As shown in Author Response Figure 3A-B, unlike neutrophils, the overall densities of $CD8^+$ T cells and $CD68^+$ macrophages showed no significant statistical differences either between the treatment-naïve and neoadjuvant chemotherapy groups, or between the non-relapsed and relapsed prognostic subgroups. Given the constraints of manuscript length, we chose to prioritize the most phenotypically altered and clinically impactful population (neutrophils) for in-depth exploration. However, we fully agree that the potential involvement of other immune cells is an important nuance. Following your constructive suggestion, we have added a paragraph in the Discussion section to explicitly acknowledge the role of other PRR-expressing immune cells in sensing EBV reactivation and clarified our rationale for focusing on neutrophils.

② Expression of key transcription factors in neutrophils

Following the reviewer's suggestion, we evaluated the expression changes of the four key transcription factors (BPTF, IRF7, HMGA1, and MAFF) that were specific to aging neutrophil in scRNA-seq data. As demonstrated in Author Response Figure 3C, the *in vitro* Smart-seq data from neutrophils co-cultured with 5-FU-treated SNU719 cells revealed that the majority of these core regulators (BPTF, IRF7, and HMGA1) were consistently upregulated.

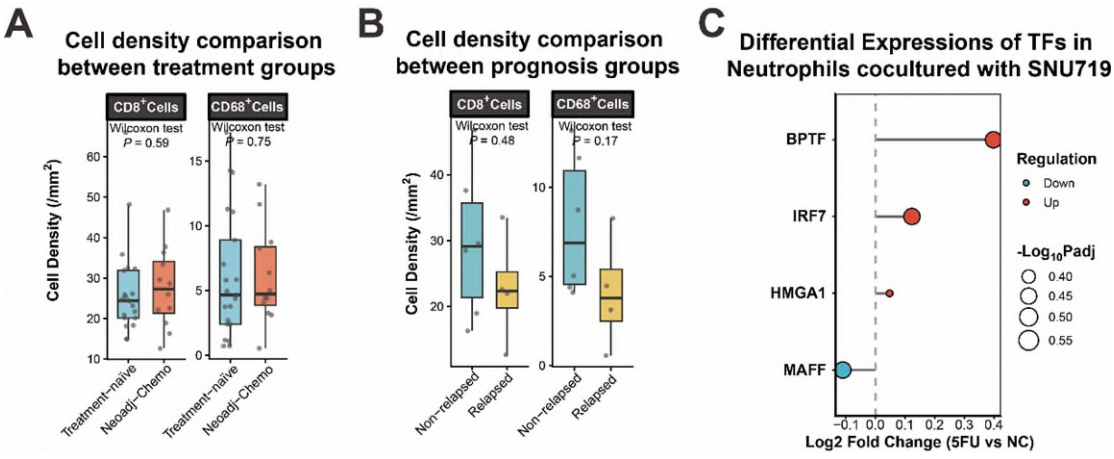

Author Response Figure 3. Validation of spatial density of $CD8^+$ T cells and $CD68^+$ macrophages at the invasive margin and neutrophil transcription factors.

A. Boxplots comparing the absolute cell density (cells/mm²) of $CD8^+$ T cells and $CD68^+$

macrophages specifically at the invasive margin between the Treatment-naïve and neoadjuvant chemotherapy (Neoadj-Chemo) groups (Two-sided Wilcoxon rank-sum test).
B. Boxplots comparing the absolute cell density of $CD8^+$ T cells and $CD68^+$ macrophages at the invasive margin between the Non-relapsed and Relapsed groups within the Neoadj-Chemo cohort (Two-sided Wilcoxon rank-sum test).
C. Lollipop plot displaying the differential expression (Log_2 Fold Change) of key aging neutrophil signature transcription factors (BPTF, IRF7, HMGA1, MAFF) in primary neutrophils co-cultured with 5-FU-treated SNU719 cells versus negative control (NC). Red dots indicate upregulation, while the blue dot indicates downregulation. The size of the dots represents the statistical significance (-Log_{10} adjusted P-value)..

Minor

The description of the data presented in Figure 1P is insufficient and should be explained more clearly.

Response:

To address this, we have comprehensively revised the figure legend for revised Figure 1K (former Figure 1P). In the updated description, we now clearly explain the biological significance of the colored spatial gradients (defining the tumor center versus the peritumoral stroma), the precise meaning of the TLS markers, and how this schematic serves as the methodological basis for the distance-based spatial quantification shown in Figure 1L. We believe this clearer explanation allows readers to fully understand the spatial distribution analysis presented in this section.

In Figure S6F, the analysis includes gastric cancers that are not EBV-positive. Therefore, the interpretation of these data in the specific context of EBVaGC should be made with caution.

Response:

We completely agree that including non-EBV-positive gastric cancer data complicates the interpretation. Because the central theme of our manuscript revolves specifically around virus-driven alterations in the tumor microenvironment of EBVaGC, this particular dataset (former Figure S6F) does not fit well with our core focus and could lead to potential misinterpretation. Therefore, to be rigorous and concise, we have decided to delete the former Figure S6F and its corresponding text from the revised manuscript. We appreciate the reviewer's cautious perspective, which has helped us keep the manuscript strictly focused on our core findings.

In Figure S6J (neoadjuvant cohort), there appears to be no statistically significant difference. Thus, the statement that CD66b and CD20 expression are inversely correlated is not supported by the presented data and should be revised or removed.

Response:

Prompted by your insightful comment, we carefully re-evaluated the rationale for including the tissue microarray cohort data (former Figure S6G-S6J). To maintain scientific rigor and avoid drawing conclusions from unsupported or underpowered data, we have accepted the reviewer's advice and removed the statement regarding the inverse correlation and former Figure S6G-J from the supplementary materials to keep the manuscript tightly focused on high-resolution spatial analyses.

In Figure 4A, the authors should include the list of genes used to define each of the six subpopulations.

Response:

To address this, we have extracted the top 50 differentially expressed genes (ranked by adjusted p-value and average log2 fold change) that specifically define each of the six neutrophil subtypes shown in Figure 4A. These gene lists are provided as a new supplementary table (Supplementary Table S6) in the revised manuscript. We have also updated the main text to reference this new supplementary table.

For Figures 4K and 4M, appropriate isotype controls should be included.

Response:

We have now incorporated the corresponding isotype controls (Brilliant Violet 421™ Mouse IgG2a, κ Isotype Ctrl, BioLegend 400259) into our flow cytometry analysis. To ensure absolute transparency and rigor, we have added a new supplementary figure (Figure S8) to detail this: In Figure S8A, we provide the comprehensive flow cytometry gating strategy, which explicitly includes the isotype control dot plot (bottom right panel) used to precisely define the CXCR4-positive gate. In Figure S8B, we present histograms overlaying the CXCR4-BV421 fluorescence intensity (solid colors) with their respective isotype controls (light gray background) for each treatment group. These additions confirm that our gating was accurate and robustly support our previous conclusion regarding the upregulation of CXCR4. We thank the reviewer for pointing this out, as it has significantly enhanced the methodological rigor of our flow cytometry data.

Reviewer #2 (Remarks to the Author):

This manuscript compellingly investigates a novel mechanism of chemotherapy resistance by focusing on the remodeling of the immune microenvironment. It establishes a critical link between the formation of tertiary lymphoid structures (TLS) and the reactivation of the Epstein-Barr virus (EBV). Leveraging a large clinical cohort of EBVaGC to date and integrating multi-omics data, the authors demonstrate that 5-FU-based chemotherapy drives EBV lytic reactivation, which in turn triggers TLR7 signaling in neutrophils, leading to the formation of neutrophil extracellular traps (NETs) that create a physical barrier, hindering lymphocyte infiltration and compromising the anti-tumor immune response. However, several important considerations need to be addressed to strengthen the conclusions and enhance the overall robustness of the study.

Response:

We sincerely thank Reviewer #2 for the highly constructive, thorough, and insightful evaluation of our manuscript. We deeply appreciate your positive remarks regarding our cohort size, multi-omics integration, and the compelling nature of the proposed mechanism. We fully agree with your critiques, particularly the need to broaden our chemotherapeutic relevance, decouple the physical/chemical suppressive mechanisms, and rigorously address clinical selection bias.

Guided by your valuable suggestions, we have conducted additional experiments and statistical analyses to significantly strengthen our conclusions. We performed *in vitro* validations using common clinical combination agents (Oxaliplatin and Paclitaxel). The new data robustly confirm that the EBV reactivation and subsequent NET-mediated physical barricade represent a universal response to DNA-damaging/cytotoxic stress, rather than being specific to 5-FU.

We provided evidence distinguishing our observed chronologically aging neutrophil phenotype from classical ARG1-dependent PMN-MDSCs. Furthermore, by incorporating an anti-PD-1 blockade in our Transwell assays, we functionally proved that the physical exclusion by NETs is the dominant, rate-limiting barrier preventing lymphocyte infiltration, which cannot be rescued by simply blocking checkpoints. Besides, we replaced non-specific inhibitors with a highly specific TLR7 neutralizing antibody to rule out off-target effects.

Additionally, we provided *in situ* evidence in patient tissues, based on a custom 10-plex mIHC panel (panel 3: PanCK/BZLF1/CD66b/MPO/CitH3/CD20/CD23/α-SMA/CXCL12/CXCR4) in a large cohort comprising 216 strictly annotated FFPE specimens (including 38 EBVaGC and 178 EBVnGC cases), co-localizing EBV lytic reactivation with NET-releasing neutrophils specifically around arrested early-TLSs.

To eliminate clinical selection bias, we implemented propensity score matching to rigorously balance baseline tumor burdens between treatment groups. The post-matched multivariable analyses solidly re-confirm that neoadjuvant chemotherapy confers no survival benefit in EBVaGC, while IM-TLS remains a robust independent protective factor.

We firmly believe your rigorous critiques have vastly improved the clinical relevance, mechanistic precision, and statistical robustness of this manuscript. Please find our detailed point-by-point responses to your comments below.

1. The mechanistic data relies primarily on 5-FU (Figures 4 & 5), yet the clinical cohort received combination therapies involving platinum drugs (e.g., oxaliplatin, cisplatin). To enhance clinical relevance, the authors should determine whether platinum-based agents also induce EBV lytic

reactivation (e.g., BZLF1 expression) and the subsequent neutrophil aging phenotype. It is important to clarify if this mechanism is specific to 5-FU or a general response to DNA-damaging chemotherapy.

Response:

To address this, we have performed comprehensive additional *in vitro* experiments using Oxaliplatin (L-OHP) and Paclitaxel (PTX). Our new data robustly confirm that the EBV reactivation and subsequent neutrophil aging cascade is a general response to cytotoxic chemotherapy, not an artifact specific to 5-FU. Similar to 5-FU, both L-OHP and PTX significantly induced EBV lytic reactivation, as evidenced by the upregulation of BZLF1 expression in EBV positive cell lines (Figure S9E, F). Conditioned medium from L-OHP/PTX-treated EBV positive cell line significantly enhanced neutrophil migration via the CXCL12 axis (Figure S8F), successfully triggered substantial NET secretion from primary neutrophils (Figure S9C). These chemotherapeutically-induced NETs significantly hindered lymphocyte migration in transwell assays (Figure S10H).

In summary, these comprehensive validations confirm that DNA-damaging and cytotoxic agents commonly used in clinical combination regimens (5-FU, L-OHP, and PTX) universally trigger the EBV reactivation.

2. The defined "aging" phenotype shares significant overlap with polymorphonuclear myeloid-derived suppressor cells (PMN-MDSCs). The authors should explicitly compare the "aging" signature with established PMN-MDSC signatures (e.g., LOX-1 expression) and senescence markers (e.g., p16, p21, β-galactosidase activity). Besides, the current data does not sufficiently distinguish whether these cells exclusively exert immune suppression via the proposed "physical barrier" (NETs) or simultaneously through other "chemical/metabolic" mechanisms (e.g., PD-L1, Arginase-1, ROS) typical of PMN-MDSCs. Perform functional assays to decouple physical exclusion from chemical suppression or exhaustion. For instance, does the inhibition of PD-1/PD-L1 or Arginase-1 or ROS restore T-cell migration in the presence of NETs?

Response:

To explicitly address this, we have systematically compared these states at the transcriptomic, proteomic, and functional levels to functionally decouple the physical barrier from chemical/metabolic suppression. We must clarify that the "neutrophil aging" observed in our model refers primarily to chronological aging and prolonged lifespan in tissues, which is canonically characterized by the loss of L-selectin (SELL/CD62L) and the reciprocal upregulation of CXCR4. As detailed in our new gene list (Supplementary Table S6), classical PMN-MDSC markers (OLR1, ARG1) were predominantly restricted to the early acute inflammatory clusters (Neu_IL1B and Neu_MMP9). In stark contrast, aging subsets (Neu_CXCR4 and Neu_VEGFA) exhibited the canonical transcriptomic signature of chronologically aging neutrophils ($CXCR4^{hi}SELL^{lo}$).

Interestingly, we also observed robust expression of CDKN1A (p21) within the Neu_VEGFA subset. Since neutrophils are post-mitotic and do not undergo classical replicative senescence, this stress-induced p21 expression likely acts as a potent anti-apoptotic mechanism. This prolongs their lifespan within the toxic tumor microenvironment, locking them into an overactive, chronologically aging state.

Consistent with the transcriptomic data, western blot validation (Figure S9G) revealed that ARG1 expression was not upregulated in neutrophils indirectly cocultured with chemotherapeutic drugs-treated EBVaGC cells. This observation further distances our observed phenotype from the classical

ARG1-dependent metabolic suppression mechanism typical of PMN-MDSCs.

Most importantly, to rigorously answer the reviewer's question of whether the immunosuppression is exerted primarily via the physical barrier (NETs) or through immune checkpoints (e.g., PD-L1), we performed a functional uncoupling assay. We modified our *in vitro* lymphocyte transwell migration assay by incorporating an anti-PD-1 antibody (Toripalimab) to blockade classical checkpoint suppression. As demonstrated in the new Figure S10J, the addition of αPD-1 completely failed to restore T-cell migration. This critical functional assay unambiguously demonstrates that while chemical suppressive axes (like PD-L1) might exist on these aging neutrophils, the macroscopic physical exclusion mediated by viscous NETs acts as the dominant, rate-limiting barrier preventing spatial T-cell infiltration into TLSs. Simply put, blocking chemical checkpoints is functionally futile if the effector T cells are physically barricaded from entering the target microenvironment.

3. The link between 5-FU, EBV, and TLR7 requires more rigorous validation. Chemotherapy can induce the release of general danger-associated molecular patterns (DAMPs), such as mtDNA, from EBV-negative cells. To control for the effects of general cell death, the authors should consider constructing stable viral knockout or cleared cell lines. In addition, hydroxychloroquine (HCQ) is a non-specific TLR7 inhibitor that also affects autophagy. Validate the mechanism using a specific TLR7 antagonist to rule out off-target effects of HCQ.

Response:

To rigorously address both concerns and rule out the off-target effects of HCQ, we have now performed precise functional validations using a specific TLR7 neutralizing antibody (αTLR7, Ultra-LEAF™ Purified anti-human TLR7, BioLegend, Cat#376911).

Specific blockade with αTLR7 almost completely reversed the robust migration of neutrophils toward CXCL12 induced by various chemotherapies (Figure S10K) and significantly abrogated the pathological NET formation triggered by chemotherapy-treated tumor supernatants (Figure S9C). Consequently, by preventing NET formation, αTLR7 functionally reversed the NET-mediated physical exclusion, successfully restoring lymphocyte migration in the transwell assays (Figure S10J).

4. The evidence primarily relies on in vitro data. Although the authors acknowledge the challenges posed by the lack of immunocompetent animal models that can effectively study EBV infection, the link between viral reactivation and NETs remains somewhat weak. To enhance the evidence, it is recommended that they conduct multiple immunohistochemistry (mIHC) analyses on NAC-treated tumor sections to co-localize EBV lytic antigens (e.g., BZLF1) with neutrophil/NET markers (CitH3, MPO) within the same microanatomical regions.

Response:

To bridge this gap and provide definitive *in situ* evidence, we performed the recommended mIHC analyses (panel 3) to spatially co-localize EBV lytic reactivation (BZLF1) with NET-releasing neutrophils ($CD66b^+MPO^+CitH3^+$) alongside TLS architectures (revised Figure 5J). The spatial imaging vividly demonstrates a striking accumulation of NET-releasing neutrophils precisely at the periphery of early IM-TLSs (IM-eTLSs), strictly accompanied by the presence of adjacent $BZLF1^+$ tumor cells. Conversely, neither the aggregation of NETs nor $BZLF1^+$ tumor cells were observed around mature IM-TLSs (IM-mTLSs). This provides intuitive, direct evidence that viral lytic

reactivation occurs in the exact same microanatomical niche as NET formation.

Beyond visual colocalization, we implemented an integrated quantitative spatial pipeline to measure the physical distances and correlations among EBV reactivation, NET density, and TLS maturation at the tumor invasive margin. As shown in revised Figure 5K, in the post-neoadjuvant chemotherapy cohort stratified by prognosis, the relapsed group exhibited a significant positive correlation between the proportion of $BZLF1^+$ tumor cells and the density of NET-releasing neutrophils. Importantly, the TLS maturity (ratio of mTLS area to total TLS area) was significantly negatively correlated with both factors. Notably, these pathogenic correlations were absent in the non-relapsed group.

By calculating exact Euclidean distances, we found that the spatial distance between NET-releasing neutrophils and $BZLF1^+$ tumor cells was significantly shorter than their distance to $BZLF1^-$ tumor cells (Figure S10D). Furthermore, a concentric spatial gradient analysis centered on NET-releasing neutrophils demonstrated that the proportion of $BZLF1^+$ tumor cells peaked in their immediate, paracrine vicinity (0–20 μm) and gradually declined further away (Figure S10E).

In the post-NAC relapsed EBVaGC group, the density of NET-releasing neutrophils at the immediate periphery (within ±100 μm) of eTLSs was significantly higher than that around mTLSs (Figure S10F). Strikingly, while this trend was also observed in non-relapsed and treatment-naïve EBVaGC patients, it was completely absent in the EBVnGC cohorts. This acts as a perfect negative control, proving that the accumulation of NETs around arrested TLSs is profoundly EBV-dependent.

Together, these newly integrated spatial and quantitative analyses strongly overcome the limitations of *in vitro* models. They provide irrefutable in situ human evidence that chemotherapy-induced EBV reactivation spatially triggers NET formation, which physically barricades the immediate microenvironment and impairs TLS maturation.

5. The retrospective comparison between NAC and surgery-upfront groups is prone to selection bias, as NAC patients often present with higher baseline tumor burden. The author should perform Propensity Score Matching (PSM) to balance baseline characteristics between the two groups. This is essential to substantiate the conclusion that NAC provides no survival benefit.

Response:

To rigorously substantiate our conclusion, we fully embraced the reviewer's suggestion and performed Propensity Score Matching (PSM) to adjust for the baseline tumor burden and clinical characteristics. The results powerfully validate our initial findings, and the detailed analyses are presented below:

As the reviewer astutely anticipated, our pre-matching analysis revealed a severe imbalance in tumor burden: 96.8% of the patients in the NAC group had clinical Stage III disease, compared to only 54.3% in the surgery-upfront group ($P<0.001$).

We then performed PSM (nearest neighbor matching, caliper = 0.2). As demonstrated in the covariate balance love plot (Author Response Figure 4A) and Author Response Table 2, the PSM successfully eliminated the selection bias. In the post-matched cohort (Control, n=31; NAC, n=25), the baseline characteristics were remarkably balanced, with clinical Stage III disease equalized at 93.5% vs. 96.0% ($P=1.000$).

Having established a balanced baseline, we re-evaluated the prognostic impact of NAC. As shown by the Kaplan-Meier curves for the matched cohort, there remained absolutely no significant overall survival (OS, $P=0.87$; Author Response Figure 4B) or disease-free survival (DFS, $P=0.87$; Author

Response Figure 4C) benefit associated with neoadjuvant chemotherapy.

Furthermore, we conducted multivariable *Cox* proportional hazards regression analyses for both OS and DFS on this matched cohort (Author Response Figure 4D, E). Strikingly, even after rigorously controlling for clinicopathological confounders, the presence of IM-TLS remained a robust and independent protective prognostic factor for DFS (HR = 0.38, 95% CI: 0.149–0.951, P = 0.039; Author Response Figure 4E). Most importantly, consistent with the Kaplan-Meier analyses, the NAC treatment itself conferred absolutely no independent survival advantage for either OS (P = 0.429) or DFS (P = 0.570).

In summary, this rigorous PSM analysis solidly substantiates our conclusion. We are deeply grateful to the reviewer for this suggestion, which has profoundly strengthened the statistical and clinical rigor of our manuscript.

Author Response Table 2. Baseline Characteristics Before and After PSM

	Before PSM			**After PSM**		
	Treatment-naive (n=70)	**Neoadjuvant Chemotherapy (n=31)**	***P* value**	**Treatment-naive (n=31)**	**Neoadjuvant Chemotherapy (n=25)**	***P* value**
Age (%)			1.000			0.749
<60	41 (58.6)	18 (58.1)		21 (67.7)	15 (60.0)	
≥60	29 (41.4)	13 (41.9)		10 (32.3)	10 (40.0)	
Sex (%)			0.808			0.499
Male	58 (82.9)	27 (87.1)		24 (77.4)	22 (88.0)	
Female	12 (17.1)	4 (12.9)		7 (22.6)	3 (12.0)	
cStage (%)			**<0.001**			1.000
II	32 (45.7)	1 (3.2)		2 (6.5)	1 (4.0)	
III	38 (54.3)	30 (96.8)		29 (93.5)	24 (96.0)	
Grade (%)			**0.040**			0.399
G1/G2	14 (20.0)	13 (41.9)		8 (25.8)	10 (40.0)	
G3	56 (80.0)	18 (58.1)		23 (74.2)	15 (60.0)	
Lauren (%)			0.994			0.809
Intestinal	13 (24.5)	5 (23.8)		3 (16.7)	3 (17.6)	
Diffuse	13 (24.5)	5 (23.8)		6 (33.3)	4 (23.5)	
Mixed	27 (50.9)	11 (52.4)		9 (50.5)	10 (58.8)	
Position (%)			**0.507**			0.510
EGJ	15 (21.4)	5 (16.1)		10 (32.3)	5 (20.0)	
Fundus	10 (14.3)	3 (9.7)		4 (12.9)	3 (12.0)	
Body	28 (40.0)	11 (35.5)		12 (38.7)	9 (36.0)	
Antrum	17 (24.3)	12 (38.7)		5 (16.1)	8 (32.0)	
LVI (%)			0.483			0.766
No	36 (51.4)	19 (61.3)		15 (48.4)	14 (56.0)	
Yes	34 (48.6)	12 (38.7)		16 (51.6)	11 (44.0)	
PNI (%)			**0.024**			0.627
No	31 (44.3)	22 (71.0)		18 (58.1)	17 (68.0)	
Yes	39 (55.7)	9 (29.0)		13 (41.9)	8 (32.0)	
IM-TLS (%)			0.069			0.877

Absence	10 (14.3)	10 (32.3)	7 (22.6)	7 (28.0)
Presence	60 (85.7)	21 (67.7)	24 (77.4)	18 (72.0)

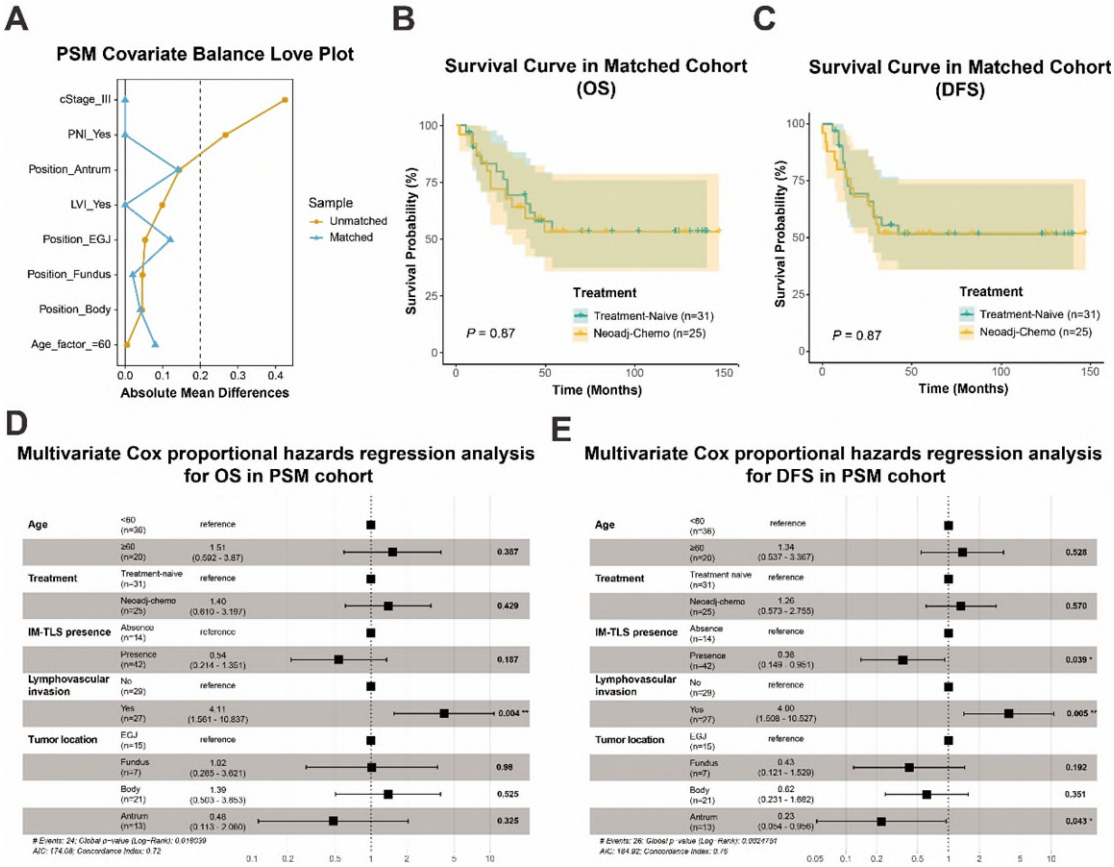

Author Response Figure 4. Survival analyses between treatment group in the PSM cohort.

(A) Love plot demonstrating the absolute standardized mean differences of clinical covariates before (Unmatched, orange circles) and after (Matched, blue triangles) propensity score matching (PSM). A threshold of 0.2 (dashed line) indicates excellent covariate balance between the two groups following PSM.

(B-C) Kaplan-Meier curves comparing Overall Survival (B) and Disease-Free Survival (C) between the matched treatment groups. Statistical significance was determined by the Log-rank test.

(D-E) Forest plots illustrating multivariable *Cox* proportional hazards regression analyses for Overall Survival (D) and Disease-Free Survival (E) within the PSM cohort.

6. The effectiveness of immune checkpoint blockade (ICB) in EBVaGC represents a promising avenue for future treatment strategies. Given the viral nature of EBVaGC and the immune landscape altered by chemotherapy, the authors should discuss the implications of their findings for the enhancement of responses to existing ICBs.

Response:

We strongly agree that exploring how our findings can inform and enhance ICB strategies is of paramount clinical significance, especially given the distinct viral and immune landscape of EBVaGC. Guided by your comment, we have carefully considered the implications of our study on ICB efficacy and have expanded our Discussion accordingly.

Reviewer #3 (Remarks to the Author):

This manuscript investigates the impact of neoadjuvant chemotherapy on tertiary lymphoid structures (TLSs) in Epstein–Barr virus–associated gastric cancer (EBVaGC). Using a large single-center cohort combined with spatial transcriptomics, single-cell RNA sequencing, multiplex immunohistochemistry, and functional in vitro assays, the authors demonstrate that neoadjuvant chemotherapy fails to improve clinical outcomes in EBVaGC and instead disrupts invasive-margin TLSs (IM-TLSs). Mechanistically, chemotherapy induces EBV reactivation, which promotes neutrophil aging via PRR activation and CXCR4–CXCL12–mediated recruitment. These aging neutrophils form NETs around TLSs, impairing lymphocyte trafficking and TLS maturation, ultimately compromising anti-tumor immunity.

The study addresses an important and timely question at the intersection of tumor immunology, viral oncology, and treatment resistance. The presented data are interesting, and the proposed link between EBV reactivation, neutrophil aging, and TLS impairment is novel and potentially impactful. However, the manuscript is very dense, and several conceptual, methodological, and presentation-related issues should be addressed to strengthen clarity, rigor, and interpretability, particularly given that the conclusions are predominantly supported by large-scale correlative omics analyses rather than direct mechanistic evidence.

Response:

We sincerely thank Reviewer #3 for the profound, visionary, and highly rigorous evaluation of our manuscript. We deeply appreciate your acknowledgement of the novelty and potential impact of our study. We fully agree with your critical assessment, particularly regarding the need for stronger *in situ* causal evidence, conceptual clarity between aging neutrophils and PMN-MDSCs, and the elimination of clinical baseline confounders. Guided by your exceptional suggestions, we have integrated large-scale spatial pathology, functional uncoupling assays, and rigorous statistical matching into this revision. The major improvements include:

To overcome the limitations of *in vitro* models, we performed large-scale quantitative mIHC on patient tissues. We provided definitive spatial evidence co-localizing EBV lytic reactivation strictly with NET accumulation at the periphery of arrested early IM-TLSs. Furthermore, by incorporating anti-PD-1 in our Transwell assays, we successfully decoupled the suppressive mechanisms, proving that the macroscopic physical exclusion by NETs—rather than checkpoint suppression—is the dominant barrier impairing lymphocyte trafficking.

We have unified our terminology to "aging neutrophils" and conducted direct transcriptomic comparisons against canonical PMN-MDSC signatures. Our data demonstrate that the neutrophils in our model are driven by a distinct chronological aging and hyper-inflammatory transcriptional state, fundamentally distinguishing them from classical ARG1-dependent PMN-MDSCs.

To address the critical issue of baseline tumor burden bias, we implemented stringent Propensity Score Matching (PSM). The post-matched analyses powerfully validate that the disruption of IM-TLS is a therapy-driven event that dictates prognostic failure, entirely independent of the initial tumor stage. We have also provided the exact 95% CIs for our pCR rates and tempered our clinical claims accordingly. We validated our novel ±300 μm spatial cutoff in an independent mIHC cohort and detailed how this high-dimensional discovery can be seamlessly translated into routine clinical digital pathology workflows.

We have comprehensively restructured the manuscript, reduced informational density, and systematically audited all statistical reporting to enhance readability and rigor.
We firmly believe that your invaluable critiques have fundamentally transformed our correlative observations into a robust, clinically relevant, and mechanistically deep narrative. Please find our detailed point-by-point responses to your comments below.

Major Comments

1. Causality between EBV reactivation and TLS disruption remains poorly mechanistically supported. While the data strongly correlate chemotherapy, EBV reactivation, neutrophil aging, NET formation, and TLS impairment, direct causal evidence in vivo is lacking. All mechanistic validation is performed in vitro. There is no animal or ex vivo tissue model demonstrating that blocking EBV reactivation, CXCR4 signaling, or NET formation restores TLS maturation. My suggestions are:

• Consider adding correlative analyses in patient tissues linking EBV lytic gene expression levels with NET density and TLS maturity.

• If feasible, include pharmacologic inhibition data (e.g., DNase I, CXCR4 blockade, or PRR inhibition) in organoid- or slice-based models.

• Quantitative multiplex immunofluorescence in patient samples—incorporating established markers of TLS maturation and functon(e.g., CD4, CD8, CD21, CD23, HEVs) with NET quantification, in larger number of patients samples rather than representative images—could strengthen this aspect. In addition, these images might support the impact on TLS development in various parts of the TME. In addition, it remains unclear whether TLS disruption is a primary driver or a secondary amplifier of immune failure. Finally, TLSs are largely treated as a binary entity despite increasing evidence of functional heterogeneity, and it is unknown whether all TLS phenotypes are equally susceptible to NET-mediated disruption.

• Explicitly acknowledge this limitation earlier in results and discussion part. Other NET-mediated immunosuppressive mechanisms (e.g., protease activity, checkpoint ligand induction) should be investigated or at least discussed.

Response:

To specifically address the reviewer's excellent suggestions, we have now conducted large-scale mIHC on patient tissues. By leveraging spatial pathology, we mapped the exact *in situ* causality, addressed TLS heterogeneity, and mechanistically uncoupled the NETs' suppressive modes.

① Quantitative spatial analyses linking EBV lytic gene expression levels with NET density and TLS maturity in patient tissues

As recommended, we utilized an extensive mIHC panel incorporating EBV reactivation, NETs, and TLS maturation. We developed an integrated quantitative spatial pipeline across patient cohorts. We spatially co-localized EBV reactivation ($BZLF1^+$), NETs ($CD66b^+MPO^+CitH3^+$), and IM-TLSs. In the relapsed post-NAC cohort, the density of NET-releasing neutrophils was significantly positively correlated with the proportion of $BZLF1^+$ tumor cells, but negatively correlated with the TLS maturity (revised Figure 5K). Spatial distance analysis (Figure S10D) and concentric gradient analysis (Figure S10E) proved that $BZLF1^+$ tumor cells peak strictly within the immediate vicinity (0-20μm) of NET-releasing neutrophils, explicitly mapping the viral diffusion radius that triggers NET formation *in vivo*.

② Addressing TLS spatial and functional heterogeneity

Our data reveal that these spatially distinct TLSs exhibit profound heterogeneity in both their susceptibility to NAC -induced effects. As demonstrated in Figure 1N, while NAC generally impacts the tumor microenvironment, the structural density reduction is only statistically significant for IM-TLSs, whereas TC-TLSs maintain a relatively stable density. More importantly, this spatial heterogeneity translates directly into clinical outcomes. In our prognostic analysis within the post-NAC samples, the density of IM-TLS was significantly diminished in the relapsed group compared to the non-relapsed group. In striking contrast, TC-TLS density showed no significant difference between the relapsed and non-relapsed groups (revised Figure 1M). Therefore, our data strongly validate the reviewer's premise: The IM-TLS represents a specific, critical immune phenotype that is susceptible to NET-mediated disruption, and its localized impairment is the defining immunological driver of therapeutic failure.

③. Alternative mechanism and which is primary driver of immune failure

To address whether immunosuppression is primarily physical (NETs) or chemical (e.g., PD-L1), we incorporated an anti-PD-1 antibody (Toripalimab) into our *in vitro* lymphocyte transwell migration model. Strikingly, as demonstrated in the new Figure S10J, the addition of αPD-1 completely failed to restore T-cell migration. This unambiguously demonstrates that while secondary chemical suppressive axes exist on these aging neutrophils, the viscous physical exclusion by NETs is the dominant barrier. Simply put, blocking chemical checkpoints is functionally futile if effector T cells are physically barricaded from entering the target TLS microenvironment.

④ Our efforts to construct ex vivo EBVaGC models

We fully agree with the reviewer that without an *ex vivo* interventional model, proving direct *in vivo* causality remains a limitation. We originally attempted to vigorously establish patient-derived EBVaGC organoids using primary tissues from our existing patient-derived xenograft (PDX) models. However, we encountered two insurmountable biological bottlenecks. First, we observed an inevitable loss of the EBV episome during continuous *in vitro* culture, stripping the model of its virus-driven characteristics. Second, these specific EBVaGC primary tumor cells failed to properly self-organize into viable 3D organoid structures within Matrigel matrices. Coupled with the extremely short *in vitro* half-life of primary neutrophils, building a fully immunocompetent, virus-retaining *ex vivo* co-culture system remains a tremendous technical hurdle.

We believe this massive integration of spatial pathology and functional uncoupling deeply enriches the mechanistic framework of our study and thoroughly addresses the reviewer's conceptual concerns.

2. The conclusion that neoadjuvant chemotherapy is ineffective in EBVaGC may be overstated, as sample size for neoadjuvant EBVaGC (n=45) is modest, regimens are heterogeneous (SOX, XELOX, DOS/POS, FLOT, FOLFOX) and pathologic complete response (pCR) rate is low but confidence intervals are not provided. My suggestions are: discuss properly your findings avoiding overstatments, provide confidence intervals for pCR and survival outcomes and discuss whether specific regimens or treatment durations showed differential effects.

Response:

As requested, we have calculated the 95% confidence interval (CI) for the pCR rate. Given the low number of events (n=1) in our neoadjuvant cohort of 45 patients, we utilized the Clopper-Pearson exact method to ensure statistical accuracy. The pCR rate is 2.2%, with a 95% CI of 0.1%–11.8%. We have now added these CI values to the Results section.

All patients received standard 3-4 cycles of neoadjuvant treatment, and duration did not significantly impact the TRG outcome. Regarding the differential effects of specific regimens, we have carefully analyzed the pathological responses across different regimens. The single patient who achieved pCR (TRG-0) received the SOX regimen. When considering a broader definition of major pathological response (TRG-0 and TRG-1), we observed a total of 3 patients: 2 in the SOX group and 1 in the XELOX group. Interestingly, all these responders received oxaliplatin-based doublet chemotherapy. However, given the modest sample size and the highly uneven distribution of patients across subgroups (e.g., SOX: n=23; FLOT: n=1), we acknowledge that this study is underpowered to detect statistically significant differential effects between regimens. The overarching observation remains that the majority of EBVaGC patients (42/45, 93.3%) exhibited suboptimal responses (TRG 2–3) regardless of the specific regimen used. We have incorporated this detailed breakdown and discussion into the revised manuscript.

3. Classification of aging neutrophils. The classification of “aging neutrophils” relies primarily on CXCR4 upregulation and transcriptomic features, raising concerns regarding definitional clarity and generalizability. Direct comparison of the proposed signature with published PMN-MDSC or senescent neutrophil gene signatures would strengthen this point. Moreover, the manuscript alternates between “aging neutrophils” and PMN-MDSC–like features without clearly defining their relationship, making it unclear whether these cells are functionally equivalent to PMN-MDSCs or represent a distinct subset. The current framing risks over-interpreting a transcriptional state as a functional lineage, which has important therapeutic implications.

Finally, given that macrophages, dendritic cells, and broader antigen-presenting cell dysfunction can independently affect TLS integrity and T cell priming, it would be important to discuss or analyze the contribution of other myeloid populations within the available transcriptomic datasets.

Response:

We sincerely thank the reviewer for this highly insightful and rigorous critique.

① Discriminating aging neutrophils from PMN-MDSC

The reviewer has perceptively highlighted a crucial conceptual distinction in myeloid biology: the risk of conflating a transcriptional state (aging) with a strictly defined functional lineage (PMN-MDSCs). To rigorously address this, we have standardized our terminology, performed direct transcriptomic signature comparisons, and evaluated the contributions of other broader immune populations as suggested.

First, we apologize for the inconsistent terminology in our original draft. In the revised manuscript, we have thoroughly removed the ambiguous "PMN-MDSC-like" descriptors. We now strictly and uniformly define these cells as "aging neutrophils." Our rationale aligns with the reviewer's premise: their profound immunosuppressive consequence in this specific microenvironment is mediated physically (by NET formation driven by an aging transcriptional state), rather than through the classical enzymatic pathways (e.g., Arginase-1) that define true MDSC lineages.

To quantitatively substantiate this definition, we performed a direct comparative transcriptomic analysis using established signatures from landmark literature. We evaluated our distinct neutrophil clusters against the aging neutrophil signature (characterized by CXCR4, ICAM1, CCL3, CXCL8, BCL2A1, NFKB1) and the canonical human PMN-MDSC signature (hallmarked by OLR1/LOX-1, ARG1, IL4I1, NOS2). As clearly demonstrated in the Author Response Figure 5A and 5B, Neu_aging subsets (Neu_CXCR4, Neu_ISG15, and Neu_VEGFA) exhibits robust and highly

specific enrichment for the classical aging and hyper-inflammatory senescence signatures. In stark contrast, they show virtually no expression of strict human PMN-MDSC functional markers, such as OLR1 and ARG1. This validation unequivocally confirms the reviewer's hypothesis: we are indeed capturing a transcriptionally distinct aging state driven by microenvironmental stress, rather than an alternative MDSC lineage.

② Exploring Other Immune Cells Responding to EBV Reactivation

We completely agree that the sensing of chemotherapy-induced EBV reactivation is not biologically exclusive to neutrophils. Viral components can be recognized by various pattern recognition receptors widely expressed on broader antigen-presenting cells (APCs) which can independently affect TLS integrity.

While transcriptomic datasets can identify the presence of these APCs, to definitively capture their functional contribution to the macro-spatial integrity of TLSs, we leveraged our high-dimensional spatial mIHC cohort (Panel 1, n=38). We quantified the absolute spatial densities of $CD68^+$ macrophages at the invasive margin (±300μm). The overall density and spatial distribution of $CD68^+$ macrophages did not drastically fluctuate either following neoadjuvant chemotherapy or between distinct prognostic groups (Author Response Figure 3A, B).

This pivotal finding suggests that while these cells undoubtedly sense the virus, their population-level spatial recruitment is surprisingly stagnant. In stark contrast, neutrophils exhibit a dominant, spatially specific, and structurally catastrophic reaction by actively accumulating and forming dense NET barricades at the invasive margin immediately upon viral stress. Therefore, we mechanistically focused on neutrophils because their uniquely destructive physical response constitutes the primary structural threat to TLS assembly.

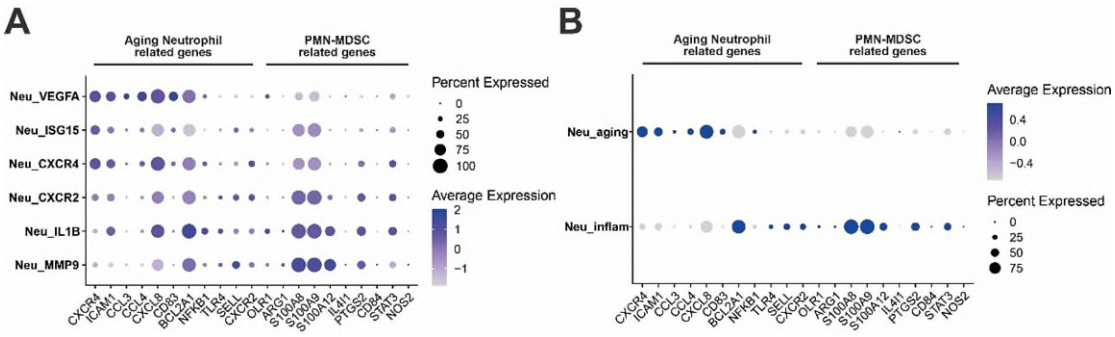

Author Response Figure 5. Single-cell transcriptomic profiling distinguishes the identified aging neutrophils from canonical PMN-MDSCs.

(A) Dot plot illustrating the expression profiles of established aging-related genes and classical PMN-MDSC-related genes across six distinct neutrophil subclusters (Neu_VEGFA, Neu_ISG15, Neu_CXCR4, Neu_CXCR2, Neu_IL1B, and Neu_MMP9).

(B) Dot plot comparing the expression of the identical gene signatures between the two broadly defined neutrophil functional states: aging neutrophils (Neu_aging) and inflammatory neutrophils (Neu_inflam).

4. Confounding effect of tumor stage and baseline immune contexture. Although the authors state that IM-TLS is an independent prognostic factor, it remains unclear whether, patients receiving neoadjuvant chemotherapy had systematically different baseline immune architectures (e.g. lower pre-existing TLS density or maturity) and/or EBVaGC tumors selected for neoadjuvant therapy were more advanced, biologically aggressive, or anatomically unfavorable.

Response:

To substantiate our conclusions and eliminate these confounding effects, we employed Propensity Score Matching (PSM) and further clarified the anatomical realities of baseline immune assessments, detailed as follows:

① Eliminating tumor stage confounders via PSM

As the reviewer astutely anticipated, our initial pre-matching analysis revealed a severe imbalance in baseline tumor burden: 96.8% of the patients in the NAC cohort presented with clinical Stage III disease, compared to only 54.3% in the upfront-surgery group ($P < 0.001$). To rectify this, we performed stringent PSM (nearest-neighbor matching, caliper = 0.2). As demonstrated in the covariate balance love plot (Author Response Figure 4A) and Author Response Table 2, the PSM successfully eradicated this selection bias. In the post-matched cohort (Treatment-naive, n=31; NAC, n=25), the clinical Stage III disease was perfectly equalized at 93.5% vs. 96.0% (P=1.000). Kaplan-Meier curves for the matched cohort confirmed that there remained absolutely no significant overall survival (OS, P=0.87; Author Response Figure 4B) or disease-free survival (DFS, P=0.87; Author Response Figure 4C) benefit associated with NAC. We conducted multivariable *Cox* proportional hazards regression on the matched cohort. Even after controlling for the balanced clinicopathological confounders, the presence of IM-TLS remained a robust, independent protective factor for DFS (HR = 0.38, 95% CI: 0.149–0.951, P = 0.039; Author Response Figure 4E).

② Addressing the "baseline immune contexture" confounder

Clinically, comprehensively evaluating the baseline TLS density prior to NAC is anatomically unfeasible. Pre-treatment tissues can only be acquired via endoscopic biopsies, which are limited to the superficial mucosa or tumor core and cannot physically sample the deep invasive margin where these critical spatial TLS architectures reside.

However, our PSM approach ingeniously addresses this biological confounder. By perfectly matching the treatment-naïve group to the NAC group, the treatment-naive group effectively serves as a highly reliable "surrogate baseline" for the natural immune contexture of locally advanced EBVaGC. Our data reveal that the upfront-surgery (surrogate baseline) samples robustly maintained intact and mature IM-TLS architectures. Therefore, the profound reduction and structural disruption of IM-TLS observed uniquely in the matched NAC cohort is not an inherent defect of their advanced stage, but rather a direct mechanistic consequence of the treatment.

In summary, PSM and spatial-anatomical logic solidly substantiate our conclusion that the disruption of IM-TLS is a therapy-driven event that dictates prognostic failure, independent of initial tumor stage. We are deeply grateful to the reviewer for prompting this analysis, which has profoundly strengthened the clinical rigor of our manuscript.

5. Spatial architecture. The redefinition of the invasive margin as a ±300 μm “functional invasive margin” based on spatial transcriptomics is an interesting and potentially important conceptual advance. However, its robustness and generalizability across samples remain unclear. The authors should clarify how sensitive their findings are to this spatial cutoff and whether alternative margin definitions or thresholds were tested. In addition, further explanation would help readers understand how this functional definition could be reproduced or approximated in routine pathological or translational settings, where spatial transcriptomic data are not readily available.

Response:

We sincerely thank the reviewer for highlighting the conceptual advance of the “functional invasive

margin" and for raising this insightful question regarding its robustness and clinical generalizability. We agree that the rationale behind this spatial cutoff and its practical translational applicability require further clarification, and we have expanded our manuscript to address these important points. To definitively address the concern regarding robustness, we tested the generalizability of this specific spatial cutoff on our independent mIHC cohort (n=23). The mIHC spatial mapping revealed that the absolute peak count of TLS falls precisely within this ±300 μm window (revised Figure S5H). As for the sensitivity of our findings to this spatial cutoff, we deliberately restricted our pathological evaluation of IM-TLS strictly to this newly defined ±300 μm functional margin in the EBVaGC cohort. Importantly, applying this specific spatial cutoff successfully stratified patient prognosis (Figure S5I). Its successful application to survival analysis serves as the ultimate proof of its robustness and its superiority as a clinically meaningful boundary.

Furthermore, this prognostic validation demonstrates exactly how our functional definition can be reproduced in routine translational settings where spatial transcriptomics data are not readily available. Once a pathologist visually identifies the morphological tumor contour on standard H&E whole slide images, standard digital pathology software (such as QuPath or ImageScope) can instantly apply a continuous, symmetrical ±300 μm digital buffer zone along the annotated margin. Pathologists or automated algorithms can then seamlessly evaluate key spatial features within this standardized 600-μm-wide ribbon. Our approach essentially bridges high-dimensional spatial discovery with cost-effective, standardizable digital pathology workflows.

Minor Comments

Clarity, structure and reporting

1) The manuscript is extremely information-dense, particularly in the Results section. Consider reducing redundancy and improving signposting to help readers follow the narrative.

Response:

We recognize that combining high-dimensional spatial pathology, single-cell transcriptomics, and *in vitro* functional assays resulted in a very dense narrative. To improve readability, we have comprehensively streamlined the Results section.

2) Some Results subsections are very long and could benefit from clearer separation of descriptive vs. mechanistic findings.

Response:

To address this, we have restructured the overly long subsections in the revised manuscript.

3) Several figures contain a large number of panels; clearer labeling and more explicit figure legends would improve accessibility.

Response:

We have carefully optimized the layout of our multi-panel figures.

4) Please ensure consistent reporting of statistical tests, sample sizes, and correction methods across figures and supplementary materials. In some places, p-values are reported without clear indication of the test used.

Response:

We have conducted a systematic and rigorous audit of all main and supplementary figure legends.

Reviewer #4 (Remarks to the Author):

In their manuscript the authors present an in-depth analysis of Epstein-Barr virus-associated gastric carcinoma (EBVaGC). Through the use of IHC, bulk RNAseq, single-cell RNAseq and spatial transcriptomics they studied tertiary lymphoid structures (TLS) in that tumor context. The authors describe TLS enrichment in EBVaGC versus EBV negative gastric carcinoma (EBVnGC), density of TLS in the invasive margin (IM) association with better prognosis and neutrophils impairing TLS maturation via NETS and the CXCR4-CXLC12 axis.

Overall, the manuscript is extremely dense with some figures even reaching panel R or S, making hard to read the labels and to properly follow the story. The authors should try to reduce the number of panels / analyses to focus their effort on analyses that directly support their claims.

Response:

We sincerely thank Reviewer #4 for the critical, constructive, and highly insightful evaluation of our manuscript. We deeply appreciate your concise summary of our work and fully accept your overarching critique regarding the density of our figures and the need for more robust, high-powered evidence to support our core mechanistic claims. Guided by your valuable suggestions, we have made substantial efforts to streamline the manuscript and rigorously validate our hypothesis:

We completely agree that the previous manuscript was overly dense. We have thoroughly reorganized our figures, removing extraneous panels (e.g., non-EBV cohorts and unsupported correlation data) and consolidating our multi-omics data to ensure the narrative focuses exclusively on analyses that directly support our central claims.

To address your critical concern regarding the limited sample size in our spatial transcriptomics, we have fundamentally scaled up our spatial analysis. We constructed a comprehensive cohort of 216 strictly annotated FFPE specimens (including 38 EBVaGC and 178 EBVnGC cases) and utilized mIHC to spatially co-localize EBV reactivation, NETs, and TLS maturation states. These high-powered quantitative spatial analyses now definitively demonstrate that NET-releasing neutrophils preferentially and physically encase early, immature TLSs at the invasive margin—a phenomenon specifically correlated with poor clinical outcomes.

To disentangle the classical immunosuppressive effects of neutrophils from their specific impact on TLS maturation, we performed targeted functional uncoupling assays. Our data explicitly differentiate this aging neutrophil phenotype from canonical ARG1-dependent metabolic or checkpoint-mediated suppression.

We are grateful for your critiques. These additions have transformed the rigor and evidentiary power of our manuscript. Please find our detailed point-by-point responses to your comments below.

Please find major comments below:

1) While it is nicely demonstrated that neo-adjuvant chemo impairs TLS maturation in EBVaGC in both IM and TC, the link with neutrophils and relapse is less convincing. The authors base this critical part of the paper on only two patients (ST data for relapsed neoadj chemo n=2). The authors should leverage the “largest cohort of patients with locally advanced EBVaGC to date” to robustly quantify neutrophils and evaluate their impact on TLS maturation and relapsed status with an appropriate number of patients.

2) Similarly, the claim that Nets producing neutrophils impairing TLS maturation in the IM, should be investigated with enough power as well. What proportion of immature TLS have Nets? Are there

mature TLS with NETs? Do patients with TLS and NETs have worse outcome? The authors should try to disentangle they well known immunosuppressor effect of neutrophils (are usually anti-correlated with B cells, T cells etc…) from there impact on TLS maturation.

Response:

We deeply appreciate this critical and constructive critique. To definitively address these vital concerns, we have fundamentally scaled up our spatial analysis and performed functional uncoupling assays. Our detailed responses are as follows:

① Streamlining figures and main text

We have reduced the number of panels in the main figures. Exploratory analyses and data not strictly essential to the main mechanism have been removed. Overly large figures have been reorganized into more digestible visual units. We have heavily edited the Results section, removing redundant descriptive summaries of single-cell data. The narrative is now tightly focused on main axis. We believe these revisions have vastly improved the readability and accessibility of our story.

② Validating hypothesis in a larger cohort (mIHC)

To achieve the requisite statistical power, we constructed a comprehensive large-scale cohort containing 216 gastric cancer FFPE specimens (including 23 whole sections and 6 TMAs). This precisely annotated cohort comprises 38 EBVaGC cases (23 neoadjuvant, 14 treatment-naïve) and 178 EBVnGC cases (40 neoadjuvant, 139 treatment-naïve). We performed mIHC to spatially co-localize EBV reactivation ($BZLF1^+$), NET-releasing neutrophils ($CD66b^+MPO^+CitH3^+$), and IM-TLS maturation states.

As visually demonstrated in revised Figure 5J, dense NET-releasing neutrophils severely accumulate precisely at the periphery of early IM-TLSs (IM-eTLSs). Conversely, these NET barricades are strikingly absent around mature IM-TLSs (IM-mTLSs). To quantify, we analyzed the NET density within a ±100μm boundary of varying TLSs (Figure S10F). In the post-neoadjuvant EBVaGC group, the density of NETs surrounding eTLSs was significantly higher than that around mTLSs. This physical encasement trend is entirely specific to EBVaGC and completely absent in EBVnGC groups. This directly proves that massive NET formation is fundamentally linked to the immature TLS state.

Spatial gradient and nearest-neighbor distance analyses confirmed that $BZLF1^+$ tumor cells are physically closest to NET-releasing neutrophils (peaking within a 0-20μm immediate vicinity; Figure S10D, E). This robustly links viral reactivation to localized NET formation at the invasive margin.

In our integrated correlation analysis within the post-neoadjuvant cohort (revised Figure 5K), the clinically relapsed group exhibited a significant positive correlation between $BZLF1^+$ tumor cells and NET density, but a profound negative correlation between NET density and the TLS maturation ratio (mTLS area / total TLS area). Notably, these pathological correlations were completely absent in the non-relapsed group.

These robust quantifications from the large cohort now definitively confirm that local EBV-driven NET formation physically stalls TLS maturation, driving clinical relapse.

③ Disentangling the physical impairment from general immunosuppression

To rigorously disentangle these two mechanisms (Chemical vs. Physical), we provided two lines of evidence. We first evaluated whether these cells behave like classical PMN-MDSCs. Western blot validation (Figure S9G) revealed that Arginase-1 expression was not upregulated in neutrophils following our specific chemotherapeutic treatment model, distancing our phenotype from classical

ARG1-dependent metabolic suppression.

To determine if the suppression is primarily a physical barricade preventing spatial assembly (TLS maturation requires T/B cell influx) or a chemical immune checkpoint, we incorporated the anti-PD-1 antibody (Toripalimab) into our *in vitro* lymphocyte transwell migration model. As demonstrated in the new Figure S10J, the addition of αPD-1 failed to restore T cell migration through the NET layer. This critical functional assay disentangles the mechanisms: while secondary chemical suppressive axes (like PD-L1) might exist on these aging neutrophils, the macroscopic physical exclusion mediated by highly viscous NETs acts as the primary, rate-limiting barrier preventing spatial T-cell infiltration.

REVIEWER COMMENTS

Reviewer #1 (Remarks to the Author):

I thank the authors for their careful and comprehensive responses to my comments. The revised manuscript has been substantially improved by the addition of functional validation experiments, an independent EBV-positive cell line, expanded spatial quantitative analyses, representative primary data, and clearer mechanistic interpretation. The authors have also appropriately revised or removed unsupported analyses and have addressed the major concerns raised during review.

Overall, I consider that the revised manuscript adequately addresses my previous concerns. I have no further major comments and support publication.

Response:

We thank you for your generous and encouraging assessment of the revised manuscript, and for taking the time to carefully evaluate our responses. We are pleased that the additional experiments and analyses have adequately addressed your concerns, and we appreciate your support for publication.

Reviewer #2 (Remarks to the Author):

The authors have fully addressed my previous comments. The manuscript is significantly improved and ready for publication. I recommend acceptance.

Response:

We thank you for your thorough re-evaluation of the revised manuscript and for your kind recommendation. We greatly appreciate your constructive engagement throughout the review process, which has helped strengthen the work considerably.

Reviewer #3 (Remarks to the Author):

The revised manuscript has been substantially improved and many of the concerns raised in the previous round have been addressed. In particular, the addition of spatial mIHC analyses, validation in an independent EBV-positive cell line, clarification of the aging neutrophil phenotype, and implementation of propensity score matching have strengthened both the mechanistic and clinical aspects of the study.

However, several points should still be considered to further strengthen the central conclusions and improve the interpretation of the data.

Response：

We sincerely thank you for the continued careful and constructive evaluation of our manuscript. In response to the three remaining comments, we have performed additional quantitative spatial analyses of NET distribution across TLS maturity stages and in relation to key TLS-associated immune populations, conducted a multivariable Cox regression analysis to assess the independent prognostic value of NET burden after adjustment for TLS-related variables, and revised the

relevant language in both the Results and Discussion sections to more explicitly distinguish data-supported observations from mechanistic interpretations. We believe these revisions have further strengthened the manuscript, and we address each comment in detail below.

1. The revised analyses provide stronger spatial evidence linking EBV reactivation, NET accumulation, and impaired TLS maturation. Nevertheless, direct evidence demonstrating that inhibition of NET formation, CXCR4 signaling, or EBV reactivation restores TLS maturation in an intact tissue context is still lacking. For this reason, some of the causal statements throughout the manuscript should be moderated.

In addition, the proposed model would benefit from a more quantitative assessment of NET distribution across different TLS maturation stages. Specifically, it would be informative to report the prevalence or density of NET-positive neutrophils in early TLSs, primary follicle-like TLSs, and secondary follicle-like TLSs. Such an analysis would provide a more direct assessment of the relationship between NET accumulation and TLS maturation. Additionally, if data are available, spatial analyses examining the relationship between NET-rich regions and the local abundance of key TLS-associated populations, particularly B cells and dendritic cells, would further strengthen the proposed mechanism.

We thank you for this constructive suggestion. We agree that a more quantitative spatial assessment of NET distribution across TLS maturity stages, as well as the relationship between NET-rich regions and key TLS-associated immune populations, would substantially strengthen the proposed mechanistic model. We have now performed the requested analyses and present the results in revised Author Response Figure 1 and revised Figure S10.

① Regarding NET density across TLS maturity stages:

We note that the original manuscript already demonstrated significantly higher NET^+ neutrophil density at the margins of immature ($CD20^+CD23^-$) versus mature ($CD20^+CD23^+$) TLS in relapsed EBVaGC patients receiving NAC, using our mIHC panel (Figure S10F). To extend this to the reviewer-requested three-category classification (E-TLS, PFL-TLS, SFL-TLS), which our mIHC panel cannot support due to the absence of CD21 staining, we performed additional H&E staining on serial sections with independent pathologist annotation. Only TLS identifiable on both sections were included, resulting in smaller sample sizes and minor numerical discrepancies relative to Fig. S10F.

NET^+ neutrophil density was quantified within the ±100 μm margin of each TLS. In relapsed EBVaGC patients receiving NAC, a decrease in NET^+ neutrophil density with increasing TLS maturity was observed (E-TLS > PFL-TLS > SFL-TLS), though comparisons did not reach statistical significance, likely due to the reduced number of TLS included after applying the paired-section criterion. In the remaining cohorts, a consistent trend of lower NET burden surrounding high-maturity SFL-TLS compared to less mature E-TLS and PFL-TLS was similarly observed (Author Response Figure 1). Collectively, these data support the association between NET accumulation and impaired TLS maturation.

② Regarding spatial relationships between NET-rich regions and TLS-associated immune populations:

Since NET-rich regions in our mIHC data could not be defined algorithmically, they were delineated manually by visual inspection of staining patterns. Representative images illustrate the morphological distinction between NET-rich and non-NET-rich areas (Figure S10G). To verify that these visually annotated regions genuinely reflect differential NET burden, we quantified

NET⁺ neutrophil density within the designated areas. As shown in Figure S10H, NET-rich regions harbored significantly higher NET⁺ neutrophil density compared to non-NET-rich regions, confirming the validity of our manual regional classification and supporting the reliability of subsequent spatial analyses based on this annotation.

Since LAMP3 (a mature DC marker) was not included in our original mIHC panel, we performed additional immunohistochemistry for LAMP3 on serial sections. Immune cell density within 0-500 µm surrounding TLS was then quantified and compared between visually annotated NET-rich and non-NET-rich regions. Representative images (Figure S10G) illustrate that CD20⁺ B cells and LAMP3⁺ DCs are preferentially found in NET-rich areas, while non-NET-rich regions lack comparable cellular aggregation. Quantitatively, LAMP3⁺ DC density was significantly higher in NET-rich regions, and CD20⁺ B cell density showed a consistent, albeit non-significant, trend in the same direction (Figure S10I). These findings suggest that NETs may physically entrap and sequester key TLS-promoting cells thereby impeding their productive contribution to TLS organization and maturation.

Taken together, these additional analyses provide a more granular quantitative and spatial characterization of the relationship between NET accumulation and TLS maturation, and further contextualize the local immune microenvironment surrounding NET-rich regions. We believe these new data collectively strengthen the mechanistic model proposed in the manuscript.

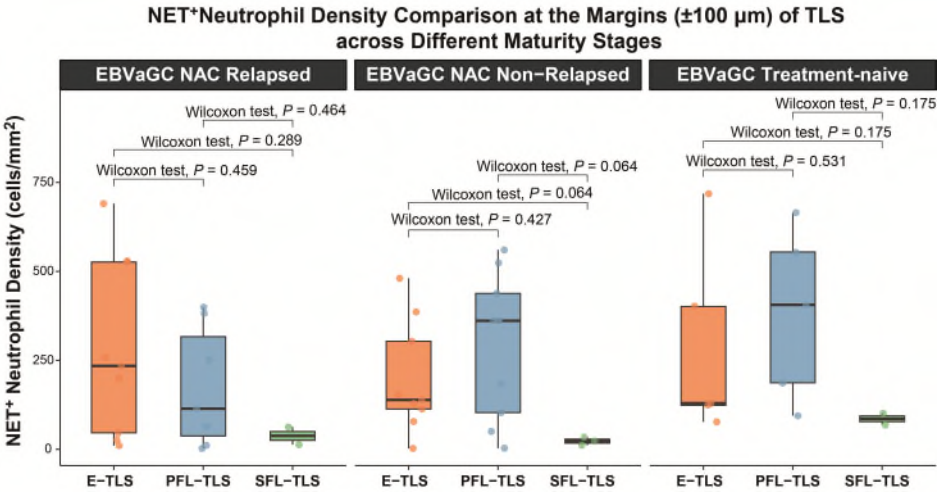

Author Response Figure 1. Spatial distribution of NETs across TLS maturity stages.

NET⁺ neutrophil density within the ±100 µm margin of TLS at different maturity stages (E-TLS, PFL-TLS, SFL-TLS) across three patient cohorts (EBVaGC NAC Relapsed, NAC Non-Relapsed, and Treatment-naive). TLS maturity was annotated by experienced pathologists on H&E-stained serial sections. Statistical comparisons were performed using the Wilcoxon signed-rank test.

2. The manuscript demonstrates associations between NET accumulation, TLS disruption, and recurrence. It would be valuable to determine whether NET burden retains prognostic significance after adjustment for TLS-related variables. If feasible, a multivariable analysis incorporating NET density together with IM-TLS status/maturity and relevant clinicopathological variables would help clarify whether NET accumulation contributes prognostic information beyond TLS measurements alone.

We thank you for this highly insightful and methodologically rigorous suggestion. This comment reflects a sophisticated understanding of the interplay between tumor immune architecture and

prognostic biomarker interpretation, and we believe that addressing it has meaningfully deepened the analytical framework of our study. We have now performed the requested multivariable analysis in our propensity score–matched (PSM) cohort (n = 56). NET^+ neutrophil density was quantified across the PSM cohort and patients were dichotomized by the median into NET-high and NET-low groups.

Kaplan–Meier analysis confirmed that NET burden was significantly associated with both OS and DFS (Author Response Figure 2A-B). We subsequently incorporated NET burden together with IM-TLS presence and other clinicopathological covariates—including age, treatment modality, lymphovascular invasion, and tumor location—into a multivariable *Cox* proportional hazard model. Upon this adjustment, the prognostic effect of NET burden was attenuated and no longer statistically significant (OS: adjusted HR = 1.66, 95% CI 0.68–4.1, $P = 0.266$; DFS: adjusted HR = 1.70, 95% CI 0.686–4.2, $P = 0.253$; Author Response Figure 2C-D). We interpret this pattern in the context of the causal framework proposed in our manuscript. Critically, we have already demonstrated that IM-TLS presence is associated with significantly lower NET^+ neutrophil density in NAC-treated patients (Fig. S10B), establishing a directional association in which NET accumulation precedes and predicts TLS maturation arrest. Jointly entering an upstream exposure (NET burden) and its downstream mediator (IM-TLS status) into the same regression model constitutes overadjustment by design; the resulting attenuation of NET's HR therefore corroborates, rather than undermines, the proposed NET → TLS disruption → recurrence pathway.

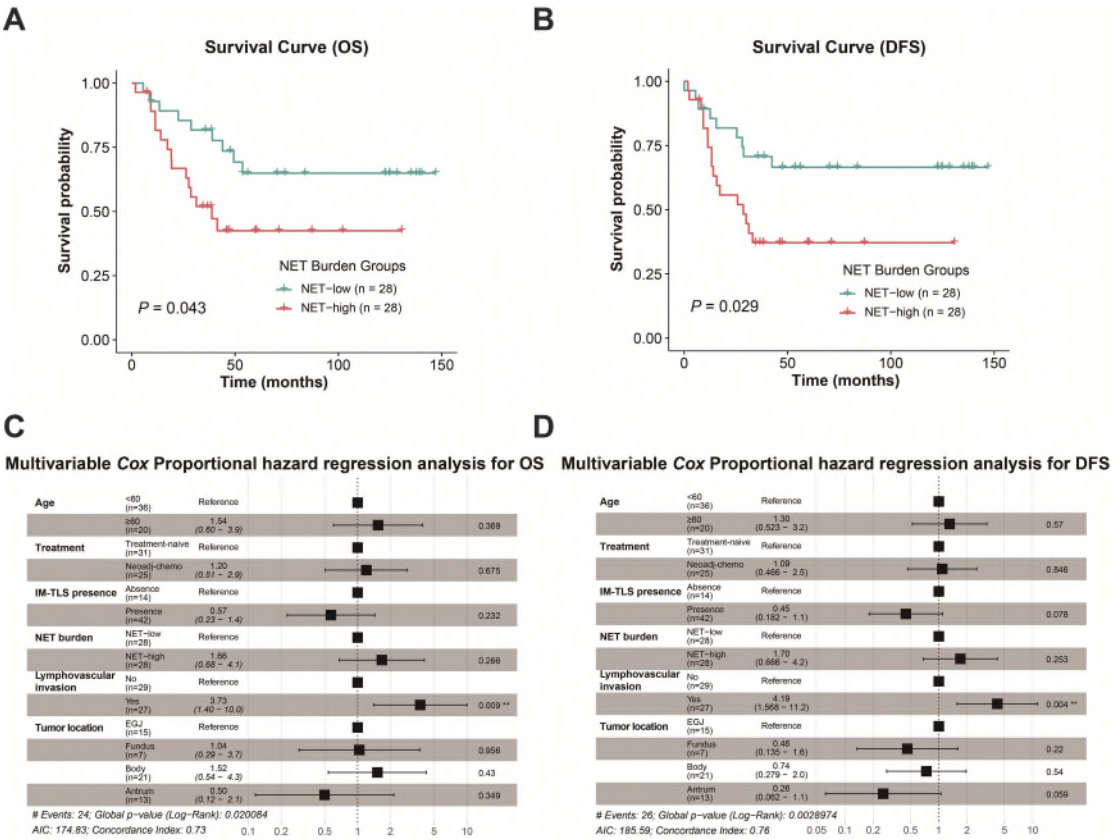

Author Response Figure 2. NET burden as a prognostic factor and its relationship with IM-TLS status in multivariable survival analysis.

(A–B) Kaplan–Meier survival curves comparing NET-high (n = 28) and NET-low (n = 28) groups in the propensity score–matched cohort for OS (A) and DFS (B). Patients were dichotomized by median NET^+ neutrophil density. Log-rank test *P* values are indicated.
(C–D) Forest plots of multivariable *Cox* proportional hazard regression analysis for OS (C) and DFS (D), incorporating NET burden, IM-TLS presence, lymphovascular invasion, tumor location, age, and treatment modality as covariates. **P < 0.01.

3. While the revised manuscript provides substantially improved spatial and mechanistic evidence, the causal relationship between NET accumulation and TLS maturation remains largely inferred from spatial associations and in vitro experiments. I encourage the authors to acknowledge this limitation more explicitly and to clearly distinguish between observations directly supported by the data and mechanistic interpretations that remain speculative.
We thank you for this constructive suggestion. We agree that explicitly delineating data-supported observations from mechanistic interpretations strengthens the manuscript's scientific rigor.
In response, we have revised the relevant language in both the Results and Discussion sections to more accurately reflect the inferential nature of the proposed NET-TLS causal axis. Specifically, language implying direct mechanistic demonstration has been moderated. Additionally, we have expanded the limitations paragraph in the Discussion to explicitly state that the causal relationship between NET accumulation and TLS maturation arrest remains inferred from correlative spatial associations and *in vitro* experimental systems, and that mechanistic interpretations regarding NET-mediated impairment of immune cell recruitment in intact tissue contexts should be regarded as hypotheses to be tested in appropriate future *in vivo* models. The specific revisions are indicated in the highlighted Revised Manuscript.
We believe these modifications appropriately temper the causal framing while preserving the integrity and novelty of the core findings.

Reviewer #4 (Remarks to the Author):

The authors have significantly improved their manuscript and appropriately addressed my comments.
Response:
We thank you for your positive re-evaluation of the revised manuscript and for your constructive comments during the review process, which have contributed to improving the work.